



3 4456 0587568 4

ORNL/TM-8364

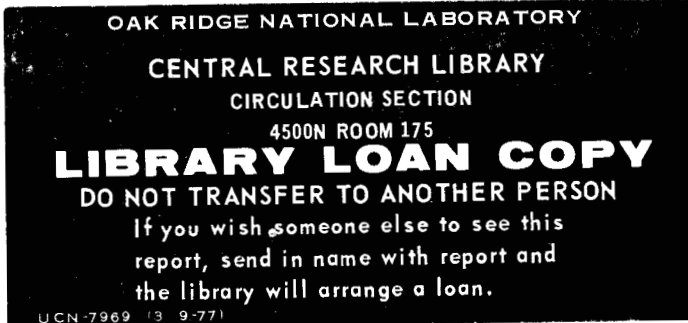
ornl

OAK
RIDGE
NATIONAL
LABORATORY

UNION
CARBIDE

Thermal/Stress Analyses of the EBT-SA Split Mirror Coil

J. A. Mayhall
G. A. Byington
J. W. Forseman
C. J. Hammonds
G. R. Haste
R. L. Johnson
J. L. Livingston



OPERATED BY
UNION CARBIDE CORPORATION
FOR THE UNITED STATES
DEPARTMENT OF ENERGY

Printed in the United States of America. Available from
National Technical Information Service
U.S. Department of Commerce
5285 Port Royal Road, Springfield, Virginia 22161
NTIS price codes—Printed Copy: A04; Microfiche A01

This report was prepared as an account of work sponsored by an agency of the United States Government. Neither the United States Government nor any agency thereof, nor any of their employees, makes any warranty, express or implied, or assumes any legal liability or responsibility for the accuracy, completeness, or usefulness of any information, apparatus, product, or process disclosed, or represents that its use would not infringe privately owned rights. Reference herein to any specific commercial product, process, or service by trade name, trademark, manufacturer, or otherwise, does not necessarily constitute or imply its endorsement, recommendation, or favoring by the United States Government or any agency thereof. The views and opinions of authors expressed herein do not necessarily state or reflect those of the United States Government or any agency thereof.

ORNL/TM-8364
Dist. Category UC-20

Contract No. W-7405-eng-26

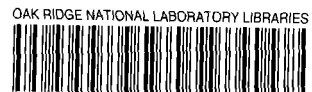
FUSION ENERGY DIVISION

THERMAL/STRESS ANALYSES OF THE EBT-SA SPLIT MIRROR COIL

J. A. Mayhall
G. A. Byington
J. W. Forseman
C. J. Hammonds
G. R. Haste
R. L. Johnson
J. L. Livingston

Date Published - June 1983

Prepared by the
OAK RIDGE NATIONAL LABORATORY
Oak Ridge, Tennessee 37830
operated by
UNION CARBIDE CORPORATION
for the
DEPARTMENT OF ENERGY



3 4456 0587568 4



CONTENTS

FOREWORD	v
1. SUMMARY	1
2. PRELIMINARY FRACTURE MECHANICS ANALYSIS	4
3. THERMAL ANALYSIS	8
3.1 ANALYTICAL MODEL	8
3.2 RESULTS	11
4. DETAILED THERMAL/STRESS ANALYSES OF THE EPOXY	11
5. THERMAL ANALYSIS WITH NO CASE COOLING	21
6. STRESS ANALYSIS	23
7. THERMAL/STRESS ANALYSIS OF NEW COOLING SYSTEM	26
8. CONCLUSIONS	29
8.1 EPOXIED COOLING TUBES	29
8.2 EFFECTS OF A NEW INTEGRALLY COOLING SCHEME	29
Appendix A: THERMAL PROPERTIES	31
Appendix B: BASELINE NASTRAN INPUT	49



FOREWORD

The following contributors were responsible for the thermal/stress analyses performed on the EBT Split-Mirror Coil:

<u>Contributor</u>	<u>Efforts</u>
Byington, G. A.	Determined convective cooling properties of the conductor and case-cooling tubes. Coordinated design, analysis, and fabrication with physicists, engineers, and craftsmen.
Forseman, J. W.	Laid out the design details.
Hammonds, C. J.	Developed the equivalent mechanical properties for NASTRAN input.
Haste, G. R.	Suggested and initiated the new cooling scheme.
Johnson, R. L.	Managed and supported the engineering work.
Livingston, J. C.	Helped develop NASTRAN thermal and stress bulk data, ran the programs, and cataloged the data.
Mayhall, J. A.	Directed NASTRAN analysis; performed fracture mechanics, stress, and thermal analysis; and wrote the report.



1. SUMMARY

A proposal was made in December 1978 to replace some of the standard mirror coils on ELMO Bumpy Torus-Scale (EBT-S) with coils which had the center windings removed, called split-mirror coils. The advantages of such a replacement were: diagnostic measurements could be made in regions in real space and in velocity space which would not otherwise be accessible, and experiments could be carried out in the high magnetic field region. The design shown in Fig. 1 was proposed to accomplish this requirement. The material selected to machine the coil was 6061-T6 Al hand forgings (because of low copper content and welding requirements). The hand forgings available from the supplier¹ were only guaranteed to have flaws smaller than 5/64 (0.078) in. Also, the inner bobbin thickness had to be thinner (in comparison with the standard coils) to meet magnetic field requirements. (The thinner bobbin should cause higher stress.) Because of the thinner bobbin and the probability of failure brought about by the possibility of 5/64-in. flaws in the material, it was necessary to perform a fracture mechanics analysis of the coil to determine whether the flaws would grow to failure during the required life² of the coil.

In order to perform a fracture mechanics analysis, the nominal stress (without flaws) has to be known, and since the thermal stress is

¹Weber Metals and Supply, MIL-I-8950B, Class B Hand Forgings inspected to Class A.

²The required life involves turning the coil on and off about 200 times. Because of uncertainties in material properties, a factor of safety of 4 should be used; i.e., required life = 800 cycles.

ORNL-DWG 82-3719 FED

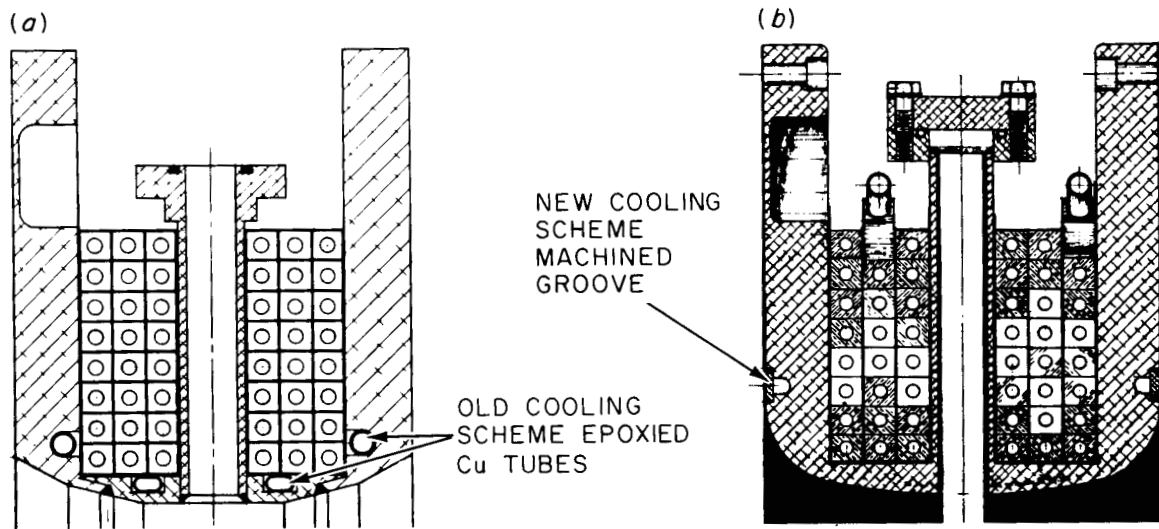


Fig. 1. Split-mirror coil - old vs new cooling scheme.

the dominating stress, the temperatures must be known in order to perform a stress analysis. Therefore, a thermal analysis was performed first. However, the expected coil temperatures (comparable to those measured with thermocouples in the in-service coils) could not be analytically attained with most probable heat-input fluxes. The measured temperatures could only be attained with the case-cooling water turned off analytically.

A detailed thermal/stress analysis of the epoxied copper cooling tube was performed, and it was found that with the conditions of case cooling, tensile stresses almost twice ultimate would be induced in the epoxy that bonds the cooling copper tube to the aluminum case. As a result, the epoxy would fail. After failure, there would be a radial gap (about 0.001 in.) between the copper tube and the epoxy, leaving only radiant heat transfer between the cooling tube and epoxy and reducing heat transfer by a calculated 95%. The only cooling left after this failure would be that due to conductor cooling; however, the heat would flow through the epoxy barrier between the conductors and case. The latter result was analyzed, and the expected temperatures were obtained (i.e., those temperatures measured with thermocouples in similar designs). It was ascertained that the epoxied cooling tubes had been failing and would fail in the new split-mirror coil.

The temperatures were determined in the coil with the failed cooling tubes, and these temperatures were used to perform the stress analysis. Stresses were found to be almost three times the yield stress (by performing a linear stress analysis) in the aluminum case; as a result, gross yielding and plastic flow were found to occur in the

6061-T6 Al. Obviously, any 5/64-in. flaw in the case would grow quickly to brittle catastrophic failure, shutting the EBT-S machine down.

A new cooling scheme was designed (as shown in Fig. 1), and temperatures and stresses were calculated. The temperatures and gradients were drastically reduced, and the maximum stress was found to be about one-half the yield stress. It was found (using fracture mechanics analysis) that the new nonepoxyed cooling scheme would ensure no failures.

2. PRELIMINARY FRACTURE MECHANICS ANALYSIS

The estimated properties for 6061-T6 Al were

$$K_{IC} @ 350^{\circ}\text{F} \cong 16.0 \text{ ksi} \sqrt{\text{in.}} , \quad (1)$$

where K_{IC} = fracture toughness value, and the crack growth rate at 350°F was

$$\frac{da}{dN} = 2.07 \times 10^{-8} (\Delta K)^{3.5} , \quad (2)$$

where

ΔK = change in stress intensity factor in $\text{ksi} \sqrt{\text{in.}}$,

a = crack length in inches,

N = number of stress cycles.

The critical crack size was

$$A_{cr} = \frac{Q}{1.21\pi M_k^2} \left(\frac{K_{IC}}{\sigma} \right)^2 , \quad (3)$$

where

A_{cr} = critical crack size,

Q = flaw-shape parameter (see Fig. 2),

M_k = magnification factor for deep flaws (see Fig. 3),

and

σ = applied stress.

Assuming σ = yield stress of 6061-T6 at 350°F after spending several hours at 350°F, or $\sigma = \sigma_y = 23$ ksi, $a/2c = 0.2$, and (from Fig. 2) $Q = 1.1$, and letting $a/t = 0.2$, then, $M_k = 1.03$ (from Fig. 3). From Eq. (3),

$$A_{cr} = \frac{1.1}{1.21\pi(1.03)^2} \left(\frac{16}{23}\right)^2 = 0.132 .$$

How many cycles are required for failure? Consider Fig. 4. The initial flaw size a_i is 0.078 in. How many stress cycles N are required for growth to $A_{cr} = 0.132$ in.²? We calculate ΔK per cycle and use Eq. (2). From Eq. (3)

$$\begin{aligned} \Delta K &= \sqrt{\frac{1.21\pi}{Q}} M_k \Delta \sigma \sqrt{a} \\ &= \sqrt{\frac{1.21\pi}{1.1}} 1.03(23.0)\sqrt{a} = 44.0 \sqrt{a} \end{aligned}$$

and from Eq. (2)

$$\frac{da}{dN} = 2.07 \times 10^{-8} (44.0)^{3.5} (a)^{3.5/2}$$

$$= 1.17 \times 10^{-2} a^{1.75} ;$$

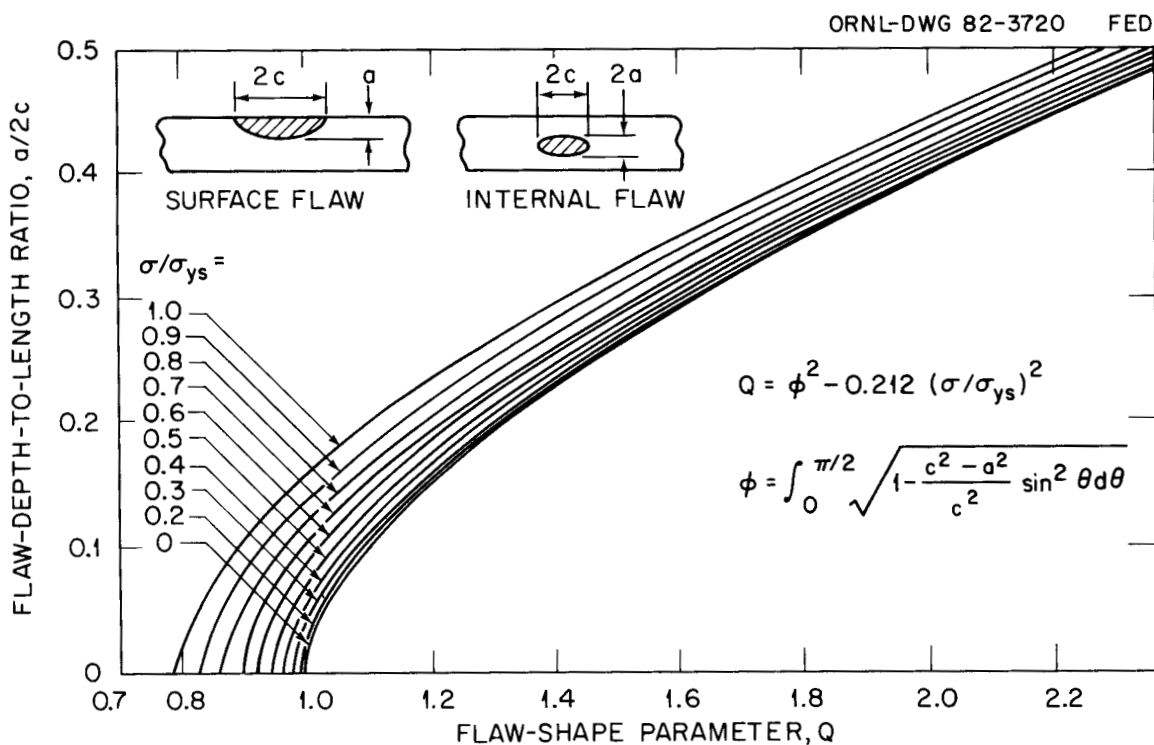


Fig. 2. Flaw-shape parameters.

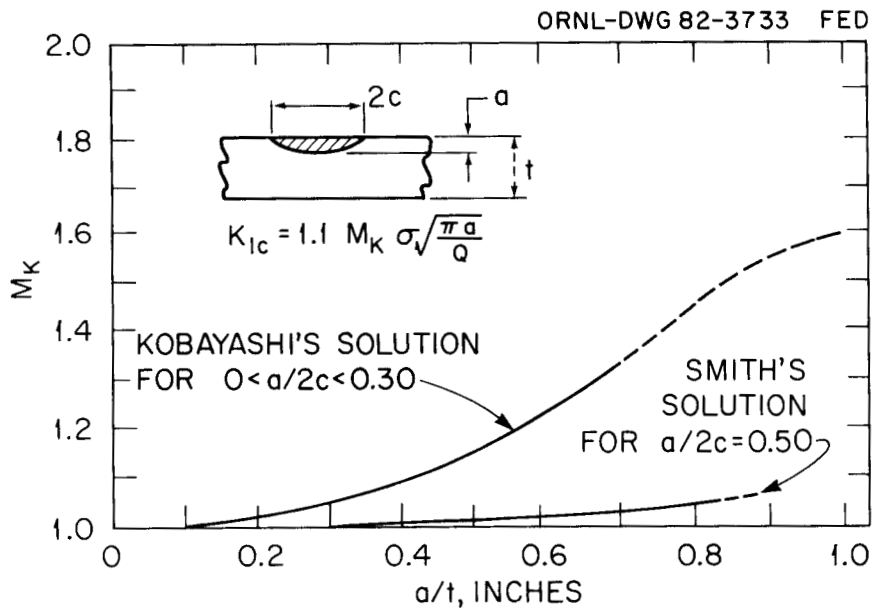


Fig. 3. Stress intensity magnification factors for deep surface flaws. (Source: Fracture Control of Metallic Pressure Vessels, NASA Report NASA SP-8040, May 1970.)

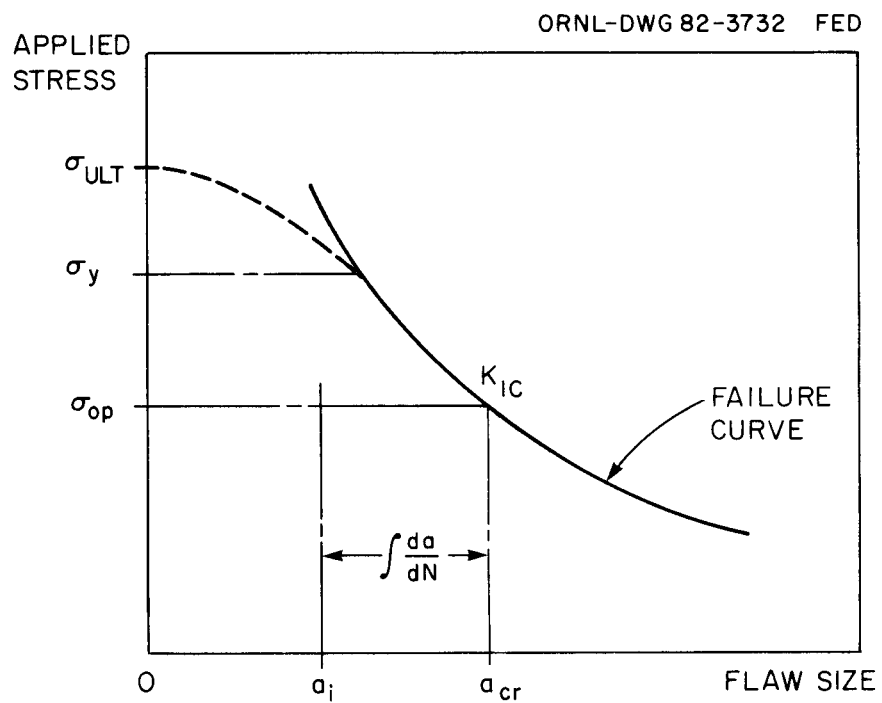


Fig. 4. Flaw size vs stress for failure.

then

$$\int_{0.078}^{0.132} a^{-1.75} da = 1.17 \times 10^{-2} \int_0^N dN ,$$

$$-\frac{1}{0.75} a^{-0.75} \left| \begin{array}{l} 0.132 \\ 0.078 \end{array} \right. = 1.17 \times 10^{-2} N ,$$

or

$$N = 114.0 \left[\frac{1}{(0.078)^{0.75}} - \frac{1}{(0.132)^{0.75}} \right]$$

$$= 252 \text{ cycles} .$$

The predicted life is 252 cycles required to fail the coil.

However, we need a life of 800 cycles, since we are not certain that the stress will not exceed yield and we do not have accurate fracture toughness data for 6061-T6. Therefore, we must perform a thermal and a stress analysis.

3. THERMAL ANALYSIS

3.1 ANALYTICAL MODEL

A NASTRAN finite-element model was developed to determine the nodal temperatures that were required for a subsequent stress analysis and fracture mechanics analysis. A computer printout plot of the NASTRAN model showing grid points is depicted in Fig. 5. The model is an axisymmetric model, using TRAPRG and TRIARG elements. Although the

ORNL-DWG 82-3734 FED

EBT MIRROR COIL HEAT LOADS
 RIGID FORMAT = 1
 RING ELEMENTS, HEAT FLOW
 UNDEFORMED SHAPE
 GRID NUMBERS

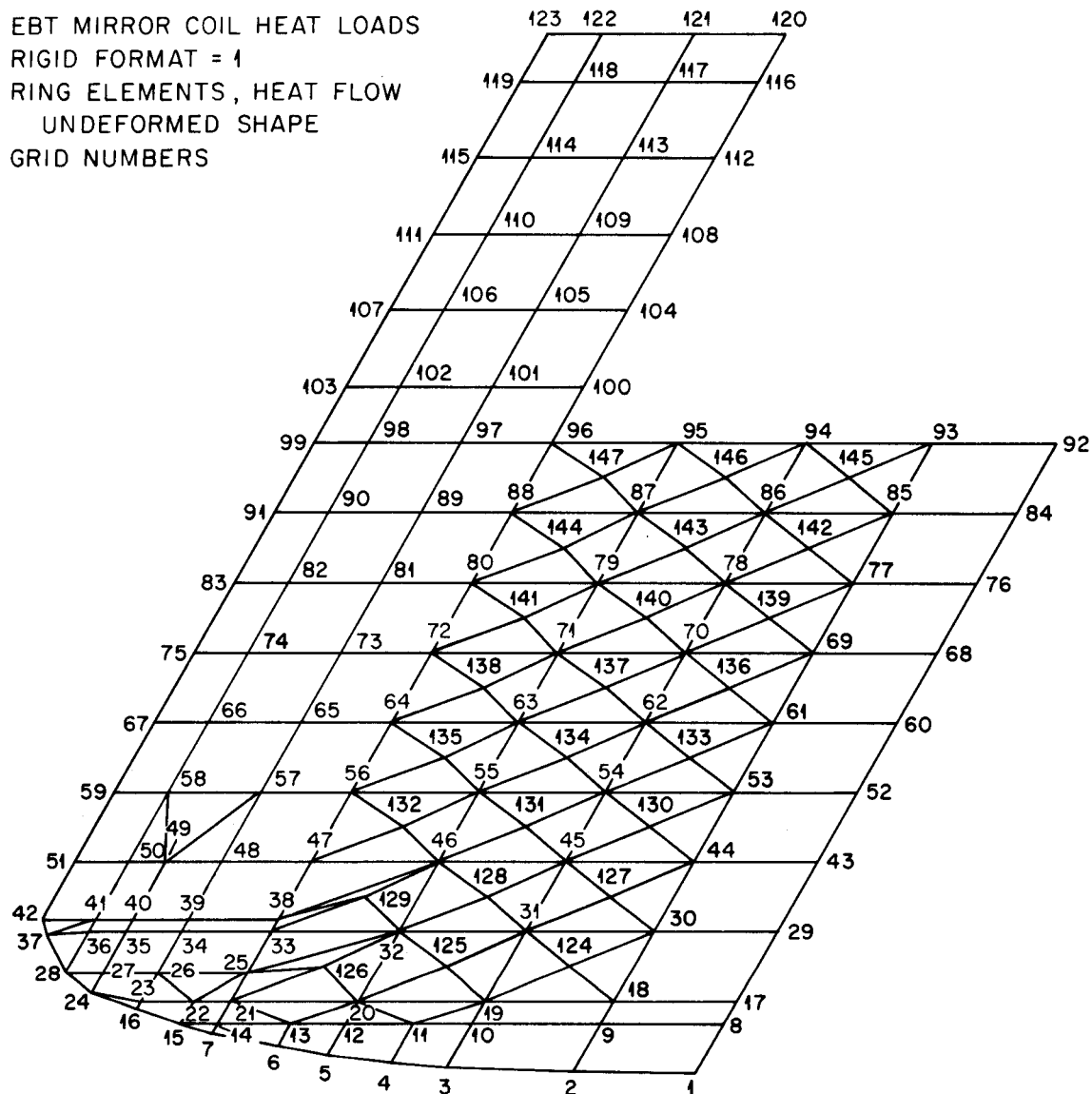


Fig. 5. Nodal grid locations.

problem is not axisymmetric, axisymmetry was assumed in order to facilitate calculations. It should be noted that the only design data given were as follows:

- (1) Approximate Maximum Temperature -- On a similarly designed EBT coil, a thermocouple was installed in the throat of the coil at a location that would be approximately at node 23 in Fig. 5. The experimentalists stated that the thermocouple was capable of measuring 200°C maximum. During several runs, it was noted that the thermocouple readout "pegged" at 200°C. The operators estimated the temperature to be somewhere between 200 and 250°C. The thermocouple was located circumferentially at a spot known to exhibit the maximum temperatures.

Since there were no available data at full power that could provide temperatures all around the circumference but there were data that provide them at the one circumferential location, we chose to assume axisymmetric distribution. This assumption made the coil hot 360° around, which gave us conservative (high) thermal hoop stresses. However, the in-plane (in the transverse direction) stresses in the hottest cross section are critical and could be accurately ascertained with an axisymmetric analysis. Therefore, we were justified in using an axisymmetric analysis. We can update our analysis and use a three-dimensional analysis if and when the temperatures are measured circumferentially.

- (2) Heat Input and Cooling Characteristics -- The total heat input to EBT-S due to plasma heating was given to be 200 kW. The basic cooling-water temperatures and manifold pressures were given, and

the coil input of I^2R heating per coil was given. Thermal properties are developed in Appendix A.

3.2 RESULTS

A baseline NASTRAN thermal analysis was performed with the coils "turned on," with no input plasma heating, and with no case cooling. The detailed NASTRAN input data for this case are shown in Appendix B. Table 1 lists the resulting calculated temperatures for this case. Note that node 23 (thermocouple location) is 111°C, and the maximum temperature is 114°C (see Fig. 6). Then, the most probable plasma heating flux (see Fig. 6) was applied, and the case cooling (at nodes 26 and 34) analytically turned on at locations shown in Fig. 1 (old cooling scheme). The resulting temperatures are indicated in Table 2. Note that the control temperature (node 23 in Table 2) rose to only 139°C. However, the operators measured over 200°C. Because of this large discrepancy, we knew something was basically wrong with the case-cooling system. Therefore, it was decided to perform a detailed thermal and stress analysis of the case-cooling system.

4. DETAILED THERMAL/STRESS ANALYSES OF THE EPOXY

The case cooling was applied in NASTRAN through element 29 as shown in Fig. 7 (by attaching equivalent convective cooling boundary elements at the nodes). A detailed "blowup" (10X size) is shown in Fig. 8; as indicated, the average temperatures T_1 and T_4 were taken from Table 2. In order to calculate stresses in the epoxy ring (around the

111°C (NODE 23)
THERMOCOUPLE
LOCATION)

POINT ID.	TYPE	TEMPERATURE VECTOR				POINT ID.	TYPE	TEMPERATURE VECTOR			
1	S	ID+1 VALUE	ID+2 VALUE	ID+3 VALUE	ID+4 VALUE	103	S	ID+1 VALUE	ID+2 VALUE	ID+3 VALUE	ID+4 VALUE
7	S	2.348469E+02	2.347710E+02	2.345135E+02	2.343334E+02	2.340469E+02	2.337400E+02	2.344121E+02	2.343298E+02	2.343249E+02	2.343249E+02
13	S	2.331512E+02	2.348790E+02	2.348091E+02	2.345285E+02	2.343288E+02	2.343288E+02	2.343288E+02	2.343288E+02	2.343288E+02	2.343288E+02
19	S	2.336982E+02	2.331060E+02	2.325436E+02	2.323714E+02	2.323603E+02	2.323603E+02	2.323603E+02	2.323603E+02	2.323603E+02	2.323603E+02
25	S	2.354476E+02	2.341792E+02	2.313648E+02	2.323556E+02	2.324503E+02	2.324503E+02	2.324503E+02	2.324503E+02	2.324503E+02	2.324503E+02
31	S	2.279703E+02	2.323294E+02	2.324102E+02	2.323264E+02	2.323264E+02	2.323264E+02	2.323264E+02	2.323264E+02	2.323264E+02	2.323264E+02
37	S	2.357953E+02	2.329241E+02	2.328701E+02	2.323264E+02	2.324733E+02	2.325752E+02	2.325752E+02	2.325752E+02	2.325752E+02	2.325752E+02
43	S	2.325655E+02	2.248667E+02	2.323294E+02	2.325198E+02	2.310344E+02	2.305613E+02	2.327627E+02	2.327627E+02	2.327627E+02	2.327627E+02
49	S	2.364984E+02	2.364703E+02	2.357912E+02	2.366899E+02	2.367141E+02	2.366899E+02	2.366899E+02	2.366899E+02	2.366899E+02	2.366899E+02
55	S	2.328398E+02	2.328705E+02	2.328880E+02	2.332277E+02	2.333268E+02	2.333268E+02	2.333268E+02	2.333268E+02	2.333268E+02	2.333268E+02
61	S	2.352080E+02	2.347128E+02	2.333605E+02	2.333905E+02	2.365475E+02	2.363390E+02	2.338924E+02	2.338924E+02	2.338924E+02	2.338924E+02
67	S	2.369721E+02	2.368374E+02	2.365475E+02	2.363390E+02	2.371533E+02	2.370506E+02	2.360279E+02	2.360279E+02	2.360279E+02	2.360279E+02
73	S	2.336720E+02	2.371453E+02	2.371014E+02	2.371533E+02	2.372514E+02	2.373054E+02	2.372625E+02	2.372625E+02	2.372625E+02	2.372625E+02
79	S	2.340114E+02	2.348752E+02	2.338534E+02	2.340127E+02	2.338656E+02	2.338420E+02	2.336581E+02	2.336581E+02	2.336581E+02	2.336581E+02
85	S	2.372362E+02	2.371318E+02	2.340127E+02	2.338656E+02	2.371614E+02	2.372613E+02	2.372016E+02	2.372016E+02	2.372016E+02	2.372016E+02
91	S	2.373427E+02	2.373363E+02	2.372833E+02	2.371614E+02	2.373202E+02	2.372772E+02	2.328266E+02	2.328266E+02	2.328266E+02	2.328266E+02
97	S	2.336343E+02	2.371422E+02	2.373117E+02	2.373202E+02	2.326557E+02	2.327723E+02	2.319206E+02	2.319206E+02	2.319206E+02	2.319206E+02
103	S	2.333764E+02	2.332566E+02	2.332304E+02	2.323347E+02	2.323500E+02	2.323622E+02	2.316184E+02	2.316184E+02	2.316184E+02	2.316184E+02
109	S	2.328349E+02	2.322932E+02	2.323347E+02	2.323500E+02	2.316364E+02	2.312764E+02	2.313331E+02	2.313331E+02	2.313331E+02	2.313331E+02
115	S	2.319517E+02	2.319561E+02	2.319466E+02	2.316137E+02	2.313491E+02	2.312764E+02	2.245100E+02	2.245100E+02	2.245100E+02	2.245100E+02
121	S	2.315937E+02	2.313993E+02	2.314994E+02	2.313491E+02	2.270534E+02	2.261729E+02	2.245407E+02	2.245407E+02	2.245407E+02	2.245407E+02
127	S	2.313396E+02	2.312579E+02	2.311377E+02	2.311377E+02	2.273823E+02	2.259492E+02	2.277372E+02	2.277372E+02	2.277372E+02	2.277372E+02
133	S	2.272335E+02	2.255671E+02	2.249193E+02	2.273823E+02	2.280050E+02	2.278876E+02	2.282110E+02	2.282110E+02	2.282110E+02	2.282110E+02
139	S	2.277079E+02	2.273127E+02	2.268949E+02	2.280445E+02	2.282386E+02	2.282110E+02	2.281408E+02	2.281408E+02	2.281408E+02	2.281408E+02
145	S	2.281690E+02	2.281251E+02	2.280445E+02	2.282215E+02	2.281181E+02	1.000000E+02	1.590000E+02	1.590000E+02	1.590000E+02	1.590000E+02

114°C (MAX)

Table 1. Nodal temperatures with coil on, no case heating or cooling

ORNL-DWG 82-3735 FED

EBT MIRROR COIL HEAT LOADS
 RIGID FORMAT = 1
 RING ELEMENTS, HEAT FLOW
 UNDEFORMED SHAPE
 ELEMENT NUMBERS

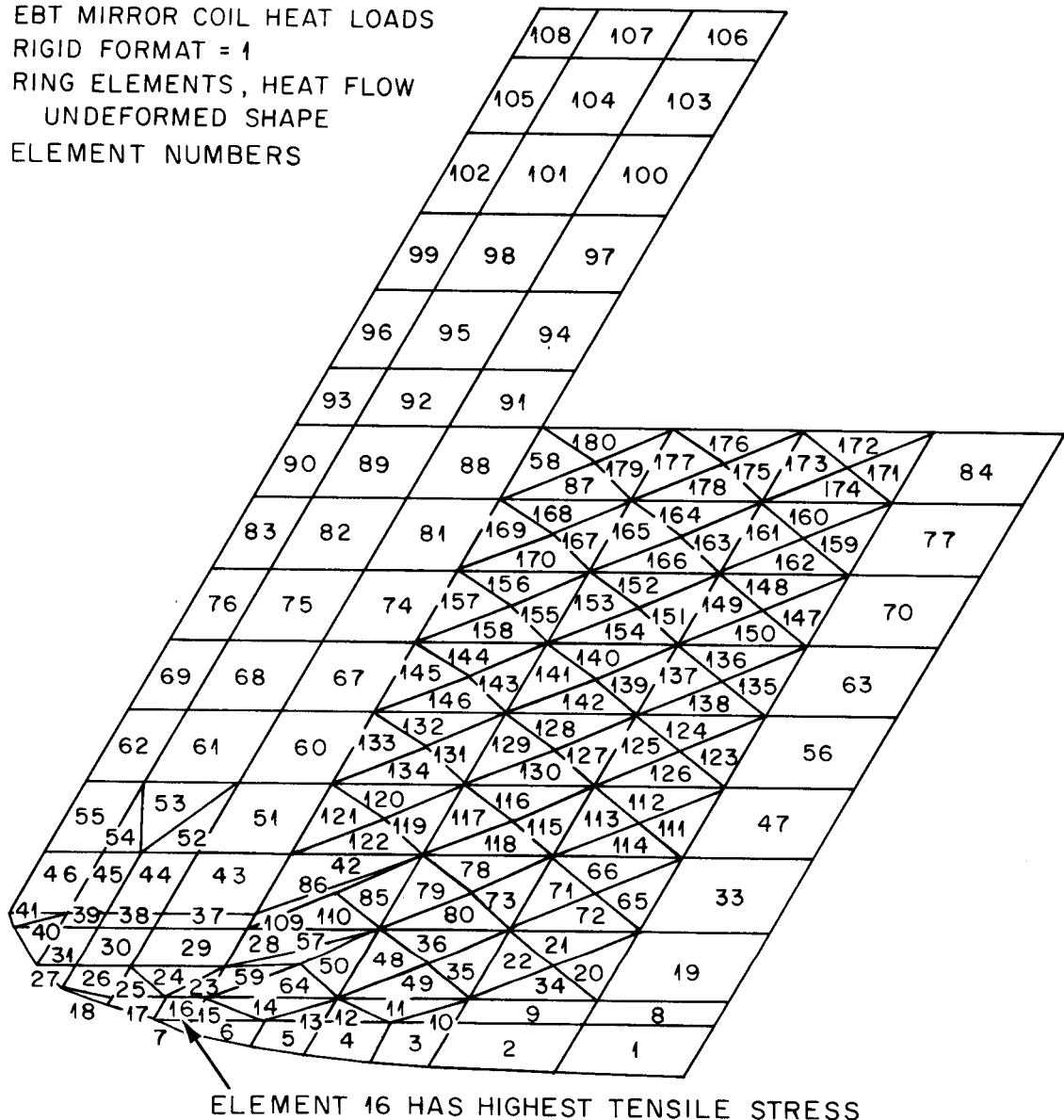


Fig. 6. NASTRAN model, showing nodes and fluxes.

POINT ID.	TYPE	TEMPERATURE VECTOR					207°C (MAX)		139°C (CONTROL)		
		ID	VALUE	ID+1	VALUE	ID+2	VALUE	ID+3	VALUE	ID+4	VALUE
1	S	2.402998E+02	2.405276E+02	2.414263E+02	2.421934E+02	2.430567E+02	2.436596E+02	2.436604E+02	2.436604E+02	2.436604E+02	2.436604E+02
7	S	2.516880E+02	2.402034E+02	2.404151E+02	2.413124E+02	2.421186E+02	2.430567E+02	2.4363955E+02	2.4363955E+02	2.4363955E+02	2.4363955E+02
13	S	2.458067E+02	2.521479E+02	2.643002E+02	2.778948E+02	2.819883E+02	2.839241E+02	2.839241E+02	2.839241E+02	2.839241E+02	2.839241E+02
19	S	2.358048E+02	2.343539E+02	2.315714E+02	2.666543E+02	2.816987E+02	2.863651E+02	2.866921E+02	2.866921E+02	2.866921E+02	2.866921E+02
25	S	2.272645E+02	1.068958E+02	1.848550E+02	4.01270E+02	1.076024E+02	3.616987E+02	3.736816E+02	3.736816E+02	3.736816E+02	3.736816E+02
31	S	2.360436E+02	2.340518E+02	2.277829E+02	2.378948E+02	3.555369E+02	3.645332E+02	3.746978E+02	3.746978E+02	3.746978E+02	3.746978E+02
37	S	3.917131E+02	2.243465E+02	1.867064E+02	3.555369E+02	2.322866E+02	3.069358E+02	3.069358E+02	3.069358E+02	3.069358E+02	3.069358E+02
43	S	2.368182E+02	2.366939E+02	2.360630E+02	2.316839E+02	2.369214E+02	2.365711E+02	2.365711E+02	2.365711E+02	2.365711E+02	2.365711E+02
49	S	3.200300E+02	3.255308E+02	3.289519E+02	2.369214E+02	3.027800E+02	3.037795E+02	2.372021E+02	2.372021E+02	2.372021E+02	2.372021E+02
55	S	2.360462E+02	2.371996E+02	2.381919E+02	2.386226E+02	2.856792E+02	2.882378E+02	2.882378E+02	2.882378E+02	2.882378E+02	2.882378E+02
61	S	2.372157E+02	2.372029E+02	2.374179E+02	2.375172E+02	2.378654E+02	2.389135E+02	2.389135E+02	2.389135E+02	2.389135E+02	2.389135E+02
67	S	2.886841E+02	2.373934E+02	2.374389E+02	2.374994E+02	2.375542E+02	2.376525E+02	2.376525E+02	2.376525E+02	2.376525E+02	2.376525E+02
73	S	2.761436E+02	2.779944E+02	2.782991E+02	2.78596E+02	2.711003E+02	2.375107E+02	2.375107E+02	2.375107E+02	2.375107E+02	2.375107E+02
79	S	2.380109E+02	2.389112E+02	2.693804E+02	2.708596E+02	2.648982E+02	2.661316E+02	2.661316E+02	2.661316E+02	2.661316E+02	2.661316E+02
85	S	2.375909E+02	2.376987E+02	2.380941E+02	2.389544E+02	2.648982E+02	2.395772E+02	2.395772E+02	2.395772E+02	2.395772E+02	2.395772E+02
91	S	2.663306E+02	2.373916E+02	2.375603E+02	2.376856E+02	2.380941E+02	2.621699E+02	2.621699E+02	2.621699E+02	2.621699E+02	2.621699E+02
97	S	2.623462E+02	2.633313E+02	2.634866E+02	2.607373E+02	2.616458E+02	2.608040E+02	2.608040E+02	2.608040E+02	2.608040E+02	2.608040E+02
103	S	2.622571E+02	2.610369E+02	2.612222E+02	2.613865E+02	2.614148E+02	2.605469E+02	2.605469E+02	2.605469E+02	2.605469E+02	2.605469E+02
109	S	2.608630E+02	2.609041E+02	2.609014E+02	2.605271E+02	2.605557E+02	2.602009E+02	2.602537E+02	2.602537E+02	2.602537E+02	2.602537E+02
115	S	2.605239E+02	2.603191E+02	2.603313E+02	2.602732E+02	2.602009E+02	2.243301E+02	2.243301E+02	2.243301E+02	2.243301E+02	2.243301E+02
121	S	2.602612E+02	2.601809E+02	2.600615E+02	2.273398E+02	2.263627E+02	2.257468E+02	2.257468E+02	2.257468E+02	2.257468E+02	2.257468E+02
127	S	2.274475E+02	2.258419E+02	2.249333E+02	2.276080E+02	2.263912E+02	2.289799E+02	2.289799E+02	2.289799E+02	2.289799E+02	2.289799E+02
133	S	2.279552E+02	2.278177E+02	2.282477E+02	2.282599E+02	2.283918E+02	2.292188E+02	2.292188E+02	2.292188E+02	2.292188E+02	2.292188E+02
139	S	2.284236E+02	2.286081E+02	2.291623E+02	2.284930E+02	2.286937E+02	1.590000E+02	1.280000E+02	1.590000E+02	1.590000E+02	1.590000E+02
145	S	2.285008E+02	2.287185E+02	2.293772E+02	2.290000E+02						

Table 2. Nodal temperatures with coil on, plasma heating on, and case cooling on

FLUX DISTRIBUTION

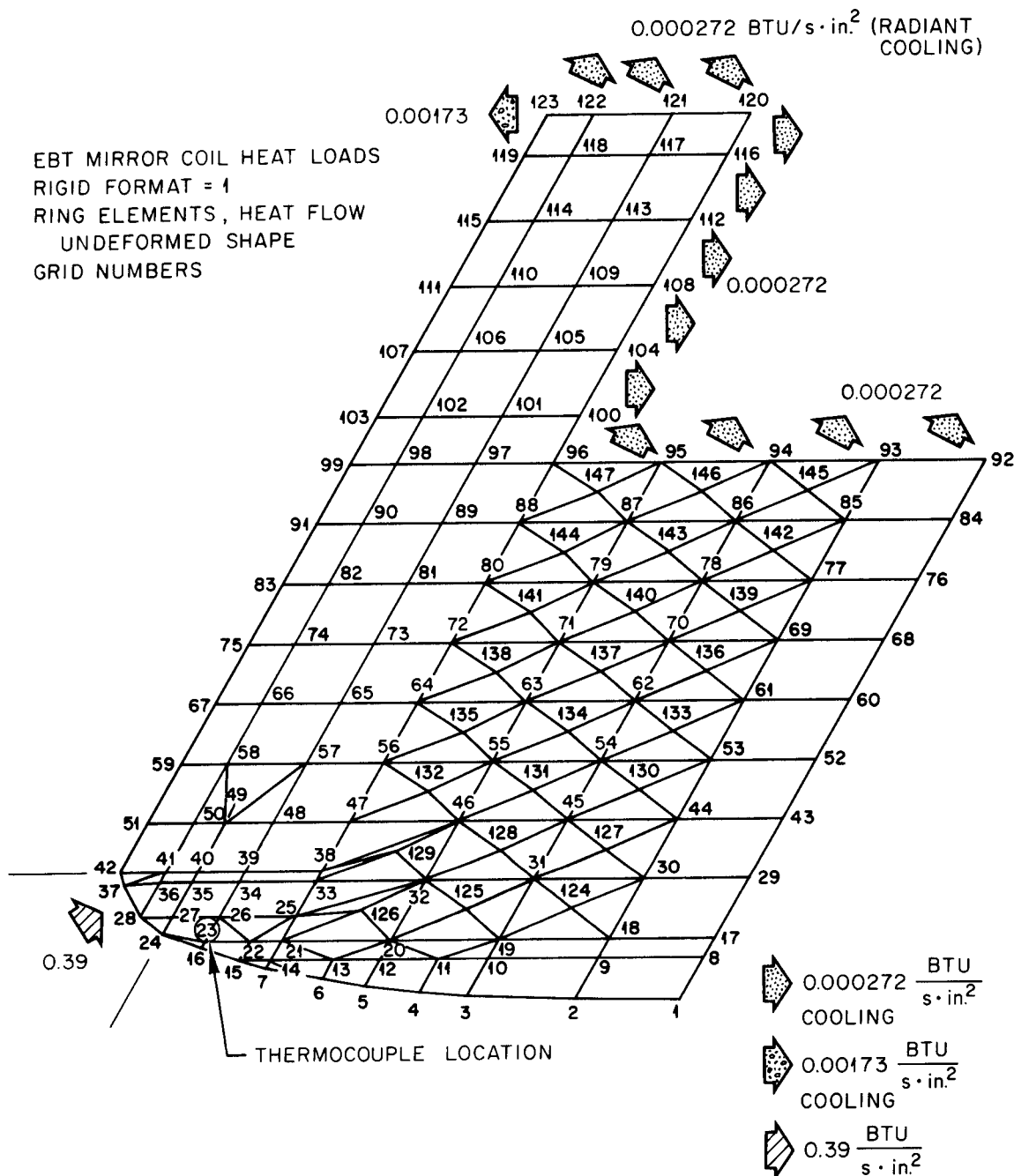


Fig. 7. NASTRAN element numbers.

ORNL-DWG 82-3736R FED

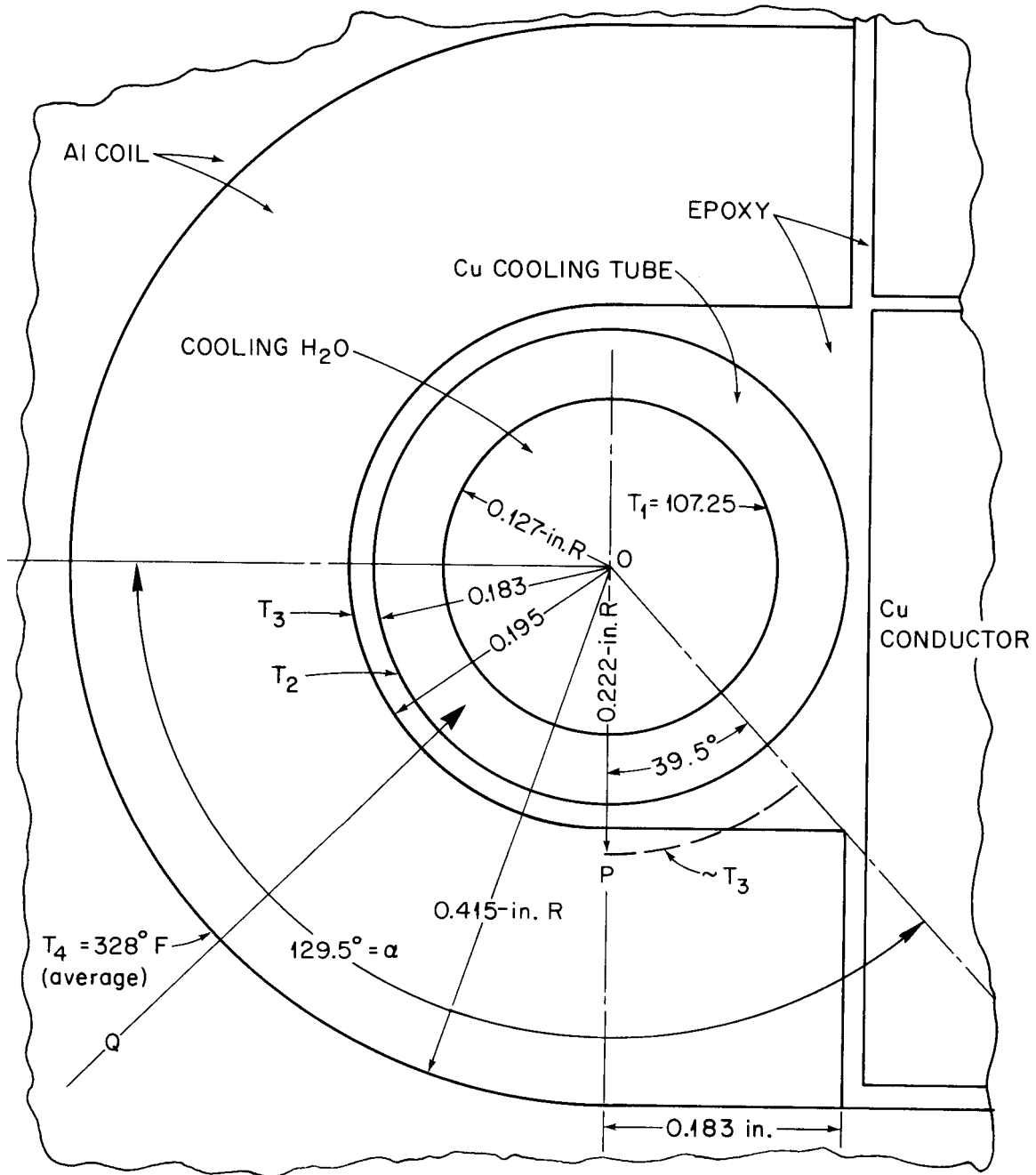


Fig. 8. Case-cooling schematic (scale: 1 in. = 0.1 in.).

cooling tube), temperatures T_2 and T_3 must be calculated by hand. (The NASTRAN model is not detailed enough.) To calculate the temperatures T_2 and T_3 , we determine the heat flow Q (Fig. 8) through the aluminum, epoxy, and copper into the cooling water over the arc length at 129.5° , using the equation

$$Q = \frac{K\Delta T}{\int_{r_i}^{r_{i+1}} dr/r\Delta\theta} = \frac{96.0(T_4 - T_3)}{\int_{0.195}^{0.415} dr/(\pi r/2)} + \frac{96.0(T_4 - T_3)}{(0.415 - 0.222)/0.183},$$

$$Q = 96.0(T_4 - T_3) \left[\frac{1}{2/\pi \ln(0.415/0.215)} + \frac{0.183}{0.193} \right],$$

or

$$Q = 320.0(328 - T_3). \quad (4)$$

Also,

$$Q = \frac{K_{\text{epoxy}}(T_3 - T_2)}{\int \frac{dr}{r\alpha}},$$

$$Q = 0.8(T_3 - T_2) \left[\frac{1}{\int_{0.183}^{0.195} dr/(\pi r/2)} + \frac{1}{\int_{0.183}^{0.222} dr/(39.5/180)} \right],$$

$$Q = 25.9(T_3 - T_2). \quad (5)$$

Finally,

$$Q = \frac{K_{Cu}(T_2 - T_1)}{\int \frac{dr}{r\Delta\theta}} = \frac{226.0(T_2 - 107.25)}{\int_{0.127}^{0.183} dr/(129.5/180)\pi r} ,$$

or

$$Q = 1398.0(T_2 - 107.25) . \quad (6)$$

Adding Eqs. (4)-(6) gives

$$Q \left(\frac{1}{320.0} + \frac{1}{25.9} + \frac{1}{1398.0} \right) = 328.0 - 107.25 ,$$

with $Q = 5200$ Btu/s/in. of circumference. Now solve Eqs. (4)-(6) for T_2 and T_3 :

$$T_3 = 328 - \frac{5200}{320} = 311.75^\circ F ,$$

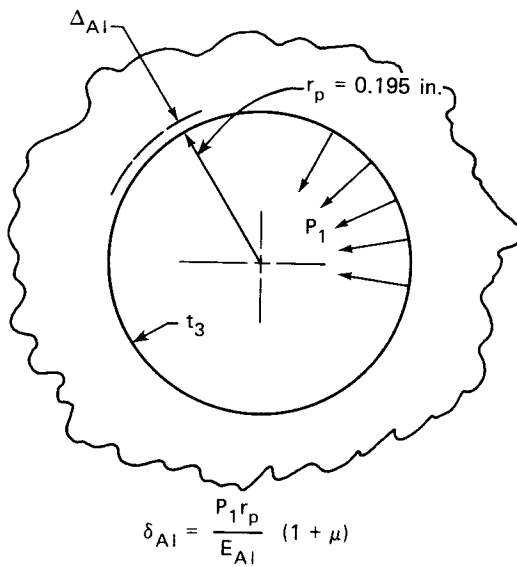
and

$$T_2 = \frac{5200}{1398} + 107.25 = 110.97^\circ F .$$

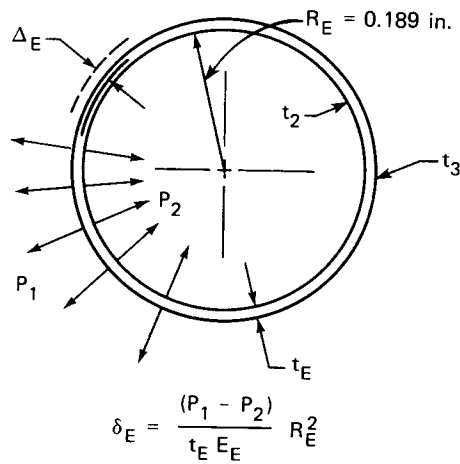
Now that we have temperatures, we will calculate the stresses in the epoxy. Consider the free-body diagrams in Fig. 9. If the copper, epoxy ring, and aluminum plate were free to expand, their expansions would be Δ_{Cu} , Δ_E , and Δ_{Al} , respectively. However, for compatibility, the stresses P_1 , P_2 , and P_3 ensure that

$$\Delta_E - \Delta_{Cu} = -S_E + S_{Cu} \quad (7)$$

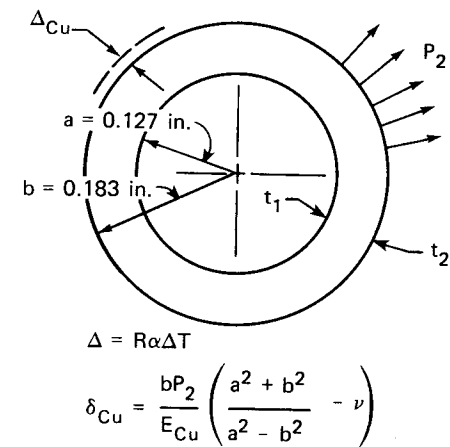
ORNL-DWG 82-3737 FED



(a) ALUMINUM PLATE



(b) EPOXY RING



(c) COPPER TUBE
 $\nu \equiv$ POISSON'S RATIO

INTERSURFACE TENSILE STRESSES $\equiv P_1, P_2$

$$\alpha_{Cu} = 9.4 \times 10^{-6} \text{ in./in.} \cdot {}^{\circ}\text{F}$$

THERMAL EXPANSIONS $\equiv \Delta_{Cu}, \Delta_E, \Delta_{Al}$

$$E_{Cu} = 17 \times 10^6 \text{ psi}$$

RADIAL DEFORMATIONS $\equiv \delta_{Cu}, \delta_E, \delta_{Al}$

$$\alpha_E = 25 \times 10^{-6} \text{ in./in.} \cdot {}^{\circ}\text{F}$$

$$E_E = 1 \times 10^6 \text{ psi}$$

$$\alpha_{Al} = 14.3 \times 10^{-6}$$

$$E_{Al} = 9.6 \times 10^6 \text{ psi AT } 312^{\circ}\text{F}$$

Fig. 9. Stresses and strains in epoxy.

and

$$\Delta_{Al} - \Delta_E = S_{Al} + S_E . \quad (8)$$

Substituting the values for the Δ 's and S 's (given in Fig. 9) into Eqs. (7) and (8), we obtain (assuming that the stress-free temperature is 70°F)

$$\begin{aligned} & 0.189 \times 25 \times 10^{-6} \left[\frac{(110.97 + 311.75)}{2} - 70 \right] \\ & - 0.183 \times 9.14 \times 10^{-6} \left[\frac{(107.25 + 110.97)}{2} - 70 \right] \\ & = -(P_1 - P_2) \frac{(0.189)^2}{0.012 \times 10^6} + \frac{0.189P_2}{17 \times 10^6} \left[\frac{(0.183)^2 + (0.127)^2}{(0.183)^2 - (0.127)^2} - 0.3 \right] \end{aligned}$$

or

$$201.78 = -P_1 + 1.00925P_2 . \quad (9)$$

Similarly,

$$2.0611 = P_1 - 0.99121P_2 . \quad (10)$$

Solving Eqs. (9) and (10), we obtain

$$P_1 = 11,200.0 \text{ psi}$$

and

$$P_2 = 11,297.0 \text{ psi} .$$

Since the ultimate tensile strength of the epoxy (STYCAST 2850 FT — a high conductivity type) is around 6000 psi, the epoxy will fail. If one were to use a higher strength epoxy (e.g., 12-14 ksi), it would probably not solve the problem because the epoxy would tend to peel away at radius \overline{op} (see Fig. 8) because of stress concentration due to non-axisymmetry of the epoxy thickness. Peel strength of an epoxy joint can be very low due to strain concentration.

In summary, we find that the calculated temperatures (Table 2) are lower than those measured experimentally because the epoxy fails and eliminates the case cooling. What kind of cooling would exist after the epoxy fails? To answer this, a radiant heat analysis was performed with a 0.001-in. gap between the copper and the epoxy. It was found that the resulting heat transfer would decrease to only 5% of what it would be before the epoxy failed. Therefore, after the epoxy fails, virtually all case cooling is eliminated.

5. THERMAL ANALYSIS WITH NO CASE COOLING

The thermal analysis was repeated with the case cooling turned off analytically, and the resulting temperatures are listed in Table 3. As noted in the table, the temperature exceeded 200°C, as expected at the thermocouple location, while the maximum temperature was 242°C. Now, to complete the analysis, a stress analysis was performed (using NASTRAN), using magnetic loads and the nodal temperatures (listed in Table 3) as thermal load.

POINT ID.	TYPE	TEMPERATURE		VECTOR		242°C (MAX)	216°C (THERMOCOUPLE)						
		ID	VALUE	ID+1	VALUE	ID+2	VALUE	ID+3	VALUE	ID+4	VALUE	ID+5	VALUL
1		2.623188E+02	2.637454E+02	2.691868E+02	2.736316E+02	2.817974E+02	2.924822E+02						
7		3.227231E+02	2.617153E+02	2.630752E+02	2.685857E+02	2.733206E+02	2.819585E+02						
13		2.933835E+02	3.250266E+02	2.823767E+02	2.109612E+02	2.427798E+02	2.389324E+02						
19		2.384673E+02	2.395650E+02	2.436507E+02	2.978159E+02	2.208374E+02	2.493367E+02						
25		2.381223E+02	4.287461E+02	4.476245E+02	4.678638E+02	2.174409E+02	2.289038E+02	2.397148E+02					
31		2.379174E+02	2.379490E+02	2.377606E+02	2.174409E+02	2.289038E+02	2.305771E+02	2.402446E+02					
37		4.574648E+02	2.333630E+02	2.124590E+02	2.223726E+02	2.2305771E+02	2.305771E+02	2.402446E+02					
43		2.381346E+02	2.376583E+02	2.373019E+02	2.338824E+02	2.380781E+02	2.815310E+02						
49		3.871235E+02	3.902104E+02	3.924631E+02	2.377469E+02	2.375520E+02	2.373800E+02						
55		2.376015E+02	2.403788E+02	3.497036E+02	3.551543E+02	2.408215E+02	2.561348E+02	2.376995E+02					
61		2.376443E+02	2.377610E+02	2.384678E+02	2.408215E+02	2.379280E+02	2.56963F+02	2.298403E+02					
67		3.305220E+02	2.377440E+02	2.377516E+02	2.379280E+02	2.386489E+02	2.4007071E+02	2.4007071E+02					
73		3.084458E+02	3.117363E+02	3.122712E+02	2.377733E+02	2.378054E+02	2.379404E+02						
79		2.386731E+02	2.403450E+02	2.964658E+02	2.991741E+02	2.996133E+02	2.377489E+02						
85		2.378146E+02	2.380090E+02	2.387511E+02	2.403612E+02	2.4087029E+02	2.909927E+02						
91		2.913611E+02	2.376198E+02	2.377765E+02	2.379902E+02	2.387657E+02	2.415729E+02						
97		2.845222E+02	2.866358E+02	2.866455E+02	2.822097E+02	2.837544E+02	2.846362E+02						
103		2.847854E+02	2.830461E+02	2.833416E+02	2.836128E+02	2.836602E+02	2.829199E+02						
109		2.830005E+02	2.830693E+02	2.830720E+02	2.826660E+02	2.826992E+02	2.826975E+02						
115		2.826760E+02	2.824629E+02	2.824766E+02	2.824204E+02	2.823486E+02	2.823486E+02						
121		2.824065E+02	2.823279E+02	2.822087E+02	2.291362E+02	2.292160E+02	2.311124E+02						
127		2.286114E+02	2.277577E+02	2.303516E+02	2.283665E+02	2.275997E+02	2.283948E+02						
133		2.284607E+02	2.286452E+02	2.299110E+02	2.286165E+02	2.289761P+02	2.301739E+02						
139		2.286974E+02	2.290660E+02	2.301166E+02	2.287275E+02	2.291045E+02	2.300876E+02						
145		2.287211E+02	2.291234E+02	2.303657E+02	1.000000E+02	1.280000E+02	1.590000E+02						

Table 3. Nodal temperatures with coil on, plasma heating off, and case cooling off

6. STRESS ANALYSIS

The maximum stresses for the case of the failed cooling tube are shown in Tables 4a and 4b. The maximum tensile stresses occur in element 16 (Table 4b, see Fig. 7 for element location). Note that this element is at the point where the case is thinnest, meaning that this would be the most probable location where failure would occur.

At element 16, the temperature would be 417°F, and the yield strength would drop to 13,080 psi. Thus, the elastically calculated stress (35,200 psi) is 2.69 times the yield stress. A repeat of the fracture mechanics analysis performed in Sect. 2 will show the following [from Eq. (3)]:

$$A_{cr} = \frac{Q}{1.21\pi M_k^2} \left(\frac{K_{IC}}{\sigma} \right)^2$$

$$A_{cr} = \frac{1.1}{1.21\pi(1.03)^2} \left(\frac{16}{35.2} \right)^2$$

or

$$A_{cr} = 0.0564 .$$

Thus, the critical crack size would reduce to 0.0564, and since the forgings can have flaws up to 0.078, one could get catastrophic failure on the first stress cycle. Obviously, we need better cooling of the coils.

EL ID	STRESS POINT	STRESSES FOR THE TRAPEZOIDAL CIRCUMFERENTIAL (THETA)				RINGS (CTR A P R G)		SHEAR (ZX)
		RADIAL (Y)	CIRCUMFERENTIAL (THETA)	AXIAL (Z)				
37	1	7.053910E+03	1.449302E+04	1.201421E+04				-2.255602E+03
	2	7.460059E+03	1.533242E+04	1.246392E+04	-5.695625E+02	-1.861785E+03	-1.753062E+03	
	3	-3.772227E+03	-1.293925E+04	-9.272305E+02	-1.496523E+03	-1.46937E+03	-2.004309E+03	
	4	-4.323328E+03	-1.415971E+04	5.513937E+03				
	5	1.604309E+03	6.822148E+02					
38	1	-1.960419E+04	-3.077787E+04	-1.685062E+03				-3.186875E+02
	2	-1.957694E+04	-3.058825E+04	-5.695625E+02	1.207644E+03	-2.056250E+03	-3.582562E+03	
	3	-7.536000E+03	-2.723900E+04	2.758937E+03	4.413937E+03	-1.187500E+03		
	4	-8.162375E+03	-2.815519E+04	2.072437E+03				
	5	-1.371962E+04	-2.918881E+04					
39	1	-1.130250E+04	-3.129537E+04	-2.914000E+03				-3.801625E+03
	2	-7.774062E+03	-2.747719E+04	2.201937E+03	-2.710065E+03	-2.162812E+03	-2.254312E+03	
	3	-3.023062E+03	-2.699656E+04	2.705125E+03				
	4	-7.445437E+03	-3.177150E+04	-3.305437E+03	-2.482250E+03			
	5	-7.384937E+03	-2.938331E+04	-3.276875E+02				
43	1	1.172435E+04	1.080097E+04	2.481526E+04				-5.282437E+03
	2	9.678469E+03	8.816406E+03	2.202279E+04	1.629437E+03	1.269750E+03	-5.642125E+03	
	3	-1.359950E+04	-2.766919E+04	-1.455481E+04	-2.405100E+04	-2.006457E+03		
	4	-2.384206E+04	-3.891219E+04	2.064937E+03				
	5	-4.003000E+03	-1.172494E+04					
44	1	-1.247456E+04	-2.754475E+04	2.473000E+03				7.985000E+02
	2	-6.439437E+03	-2.050912E+04	2.192062E+03	2.19562E+03			
	3	-5.317687E+03	-2.088519E+04	1.648750E+03	3.530000E+02	-1.048000E+03	5.757812E+02	
	4	-1.283706E+04	-2.951150E+04	4.855625E+02				
	5	-9.253625E+03	-2.456087E+04	1.703500E+03				
45	1	-1.307519E+04	-2.974969E+04	-6.993750E+01				-1.701750E+03
	2	-5.815000E+03	-2.138250E+04	4.886250E+02	1.240850E+03			
	3	-2.646125E+03	-2.040706E+04	1.330562E+03	-8.68770E+01	-3.029250E+03		
	4	-1.168650E+04	-3.071037E+04	-1.008125E+03	-8.942617E+02			
	5	-8.290312E+03	-2.552669E+04	2.006875E+02				
46	1	-1.220225E+04	-3.122637E+04	-2.212000E+03				-1.678250E+03
	2	-2.054625E+03	-1.981575E+04	2.710312E+03	8.089375E+02			
	3	-2.459937E+03	-1.792137E+04	4.340125E+03	-7.090625E+02			
	4	-1.023731E+04	-3.206775E+04	-3.131625E+03	-3.196250E+03			
	5	-5.491062E+03	-2.521667E+04	4.442500E+02	-1.193742E+03			
47	1	-8.984961E+02	2.532152E+03	4.408395E+03				-6.613672E+01
	2	-1.038715E+03	2.149422E+03	4.198586E+03	1.499853E+02			
	3	-5.470898E+02	2.408152E+03	4.489391E+03	1.545586E+02			
	4	-4.020703E+02	2.775484E+03	4.706613E+03	-6.156250E+01			
	5	-7.247227E+02	2.458586E+03	4.445848E+03	4.421753E+01			

Table 4(a). Maximum stresses with failed cooling tube

EL ID	STRESSES FOR THE TRAPEZOIDAL RINGS (CTRAPPING)					SHEAR (ZX)
	STRESS POINT	RADIAL (X)	CIRCUMFERENTIAL (THETA)	AXIAL (Z)		
16	1	-4.795812E+03	-1.898031E+04	-1.593862E+04	-1.374581E+04	
	2	-2.638413E+04	-1.263344E+04	-2.105832E+04	-1.116133E+04	
	3	-1.658237E+04	-3.510244E+04	-2.639181E+04	-8.633562E+03	
	4	-1.844437E+04	-3.625419E+04	-3.207075E+04	-1.121794E+04	
	5	-2.655562E+03	-1.955162E+04	-1.333175E+04	-1.118975E+04	
17	1	-8.552687E+03	-2.816250E+04	-1.366575E+04	-1.218106E+04	
	2	-7.812250E+03	-2.693244E+04	-5.939750E+03	-9.072219E+03	
	3	-2.082625E+03	-3.085656E+04	-8.391187E+03	-4.465562E+03	
	4	-2.231562E+03	-3.241556E+04	-1.234219E+04	-5.712812E+03	
	5	-5.435500E+03	-2.968019E+04	-1.010044E+04	-7.860250E+03	
19	1	-1.372805E+03	1.300039E+03	-9.823945E+02	4.229688E+01	
	2	-2.816412E+01	2.948512E+03	-3.802754E+03	-3.103704E+02	
	3	-6.469219E+02	2.6133301E+03	-3.487996E+03	1.096642E+03	
	4	-1.841734E+03	1.289730E+03	-9.381836E+02	1.449310E+03	
	5	-9.567656E+02	2.031691E+03	1.335371E+03	5.694741E+02	
26	1	-7.737312E+03	-3.089581E+04	-2.843312E+03	-7.487125E+03	
	2	-7.831312E+03	-3.013881E+04	-4.894375E+02	-4.230426E+03	
	3	-9.155000E+02	-3.189806E+04	-1.396437E+03	-2.756812E+03	
	4	-3.570312E+03	-3.544906E+04	-5.923687E+03	-5.248437E+03	
	5	-5.014812E+03	-3.209900E+04	-2.665062E+03	-4.928562E+03	
29	1	4.054453E+03	7.950371E+03	9.142652E+03	-2.321359E+03	
	2	-3.622383E+03	-1.155992E+03	7.863016E+03	-1.288690E+03	
	3	-1.982133E+03	-6.491223E+03	-5.871016E+02	-1.800904E+03	
	4	-2.236781E+03	-7.181437E+03	-5.900000E+01	-2.833574E+03	
	5	8.653008E+02	3.607812E+02	4.09602E+03	-2.061160E+03	
30	1	-2.690562E+04	-3.831294E+04	-8.665062E+03	-1.009225E+04	
	2	-2.023269E+04	-3.104706E+04	1.413625E+03	-1.712689E+03	
	3	-4.270000E+02	-2.484019E+04	7.727250E+03	-3.391250E+02	
	4	-1.0069062E+04	-3.582050E+04	-5.320500E+03	-8.718562E+03	
	5	-1.439900E+04	-3.248262E+04	-1.201562E+03	-5.215496E+03	
31	1	-8.256562E+03	-3.400806E+04	-1.090750E+03	-4.581000E+03	
	2	-3.567187E+03	-2.798025E+04	4.005625E+02	-5.578484E+02	
	3	-5.845000E+02	-2.833050E+04	1.355625E+02	-1.437312E+02	
	4	-7.354250E+03	-3.785437E+04	-4.605125E+03	-5.460375E+03	
	5	-4.633812E+03	-3.200919E+04	-1.275312E+03	-3.009227E+03	
33	1	-1.348891E+03	2.301598E+03	3.047992E+03	-3.103711E+02	
	2	-1.039828E+03	2.466945E+03	4.332320E+03	-6.613452E+01	
	3	-4.827422E+02	2.738266E+03	4.663164E+03	3.742344E+02	
	4	-7.611992E+02	2.580559E+03	3.426504E+03	1.300000E+02	
	5	-9.122422E+02	2.511801E+03	3.861080E+03	3.143628E+01	

Table 4(b). Maximum stresses with failed cooling tube

7. THERMAL/STRESS ANALYSIS OF NEW COOLING DESIGN

An alternative cooling scheme, suggested by Glenn Haste, is shown in Fig. 1. The results of a NASTRAN thermal analysis of the new cooling scheme are shown in Table 5. As shown, with no epoxy thermal barrier (i.e., the cooling scheme consists of a circumferential groove machined in the side of the case, covered with a welded circular strip, and fed via radial drilled holes), the nodal temperatures are drastically reduced.

Using the nodal temperatures (in Table 5) as thermal load input, a NASTRAN stress analysis was performed and the maximum stresses listed in Table 6. As noted, the maximum stress occurred in element 54 and is 15,630 psi. This is 54% of yield (28,800 psi), which is a remarkable improvement over the old design. Repeating the fracture mechanics analysis for this case and using Eq. (2), we find

$$A_{cr} = \frac{1.1}{1.21\pi(1.03)^2} \left(\frac{16}{15.63} \right)^2 = 0.288 .$$

Now using Eq. (1) to determine how many cycles are required for an initial crack size of 0.078 to grow to 0.288, from Eq. (2), we find

$$\Delta K = \sqrt{\frac{1.21\pi}{Q}} M_k \Delta \sigma \sqrt{a} ,$$

or

$$\Delta K = \sqrt{\frac{1.21\pi}{1.1}} 1.03(15.63)\sqrt{a} = 29.93 \sqrt{a} .$$

POINT ID.	TYPE	TEMPERATURE VECTOR					86.1°C						
		ID	VALUE	ID+1	VALUE	ID+2	VALUE	ID+3	VALUE	ID+4	VALUE	ID+5	VALUE
1	S	2.278804E+02	2.274356E+02	2.257787E+02	2.244676E+02	2.221221E+02	2.191526E+02						
7		2.111391E+02	2.280686E+02	2.276373E+02	2.259429E+02	2.245347E+02	2.220477E+02						
13		2.188783E+02	2.105294E+02	1.961071E+02	1.875742E+02	2.340219E+02	2.343449E+02						
19		2.3440491E+02	2.323021E+02	2.274477E+02	1.922504E+02	1.869628E+02	1.926562E+02						
25		2.244492E+02	2.349572E+02	2.322452E+02	2.248973E+02	2.353371E+02	2.357611E+02						
31		2.1584260E+02	2.210718E+02	2.1453025E+02	2.1364672E+02	2.1196512E+02	2.1414857E+02						
37		2.358668E+02	2.359469E+02	2.350620F+02	2.295211E+02	2.262341E+02	2.329078E+02						
43		2.1243418E+02	2.128943E+02	2.192556E+02	2.362278E+02	2.362420E+02	2.355893E+02						
49		2.337635E+02	2.310126E+02	2.507592E+02	2.455083E+02	2.449448E+02	2.365403E+02						
55		2.365753E+02	2.362664E+02	2.352862E+02	2.332572E+02	2.332572E+02	2.365403E+02						
61		2.1641328E+02	2.367757E+02	2.368313E+02	2.366405E+02	2.359534E+02	2.343415E+02						
67		2.1806512E+02	2.1780255E+02	2.1775987E+02	2.169069E+02	2.1696897E+02	2.168126E+02						
73		2.362271E+02	2.348494E+02	2.892288E+02	2.870280E+02	2.866713E+02	2.369301E+02						
79		2.370153E+02	2.368645E+02	2.362363E+02	2.348773E+02	2.348773E+02	2.369301E+02						
85		2.1922361E+02	2.368142E+02	2.369867E+02	2.368477E+02	2.361898E+02	2.337314E+02						
91		2.1966993E+02	2.1951764E+02	2.1949408E+02	2.1971889E+02	2.1962123E+02	2.1956715E+02						
97		2.1955804E+02	2.1958977E+02	2.1957571E+02	2.1956042E+02	2.1955757E+02	2.1953444E+02						
103		2.1953440E+02	2.1953020E+02	2.1952840E+02	2.1950035E+02	2.1950186E+02	2.1949889E+02						
109		2.1949620E+02	2.1947809E+02	2.1947895E+02	2.1947252E+02	2.1946518E+02	2.1947137E+02						
115		2.1947188E+02	2.1946343E+02	2.1945141E+02	2.1945225E+02	2.1950374E+02	2.221630E+02						
121		2.266619E+02	2.245760E+02	2.224112E+02	2.268961E+02	2.250482E+02	2.222611E+02						
127		2.272791E+02	2.264955E+02	2.249154E+02	2.276208E+02	2.271693E+02	2.260624E+02						
133		2.278160E+02	2.274781E+02	2.265887E+02	2.279009E+02	2.275832E+02	2.267580E+02						
139		2.279115E+02	2.275823E+02	2.265139E+02	2.265000E+02	2.280000E+02	2.1590000E+02						
145													

114°C (MAX)

Table 5. Nodal temperatures for new cooling scheme

EL ID	STRESS POINT	STRESSES FOR THE TRAPEZOIDAL RINGS { C T R A P R G }				SHEAR (ZX)
		RADIAL (X)	CIRCUMFERENTIAL (THETA)	AXIAL (Z)		
51	1	-1.452646E+04	-1.305621E+04	-1.342048E+04	4.176250E+02	
	2	-1.532112E+04	-1.395949E+04	-1.309480E+04	-1.155187E+03	
	3	6.316844E+03	1.013691E+04	1.105860E+04	-7.064297E+02	
	4	1.150748E+04	1.563248E+04	1.512886E+04	8.663828E+02	
	5	-3.008676E+03	-3.186172E+02	-8.507813E+01	-1.444336E+02	
55	1	7.592930E+03	1.371274E+04	3.505555E+03	1.575375E+03	
	2	-5.339844E+02	1.33266E+03	-8.711602E+02	-9.261438E+02	
	3	-4.749727E+03	2.82711E+03	-2.617902E+03	-8.67969E+01	
	4	1.268258E+03	9.942195E+03	-3.499297E+02	2.480820E+03	
	5	8.865781E+02	7.999383E+03	-9.116797E+01	7.472891E+02	
56	1	2.735156E+01	-1.373242E+02	-8.486328E+01	-1.054297E+01	
	2	-1.090625E+01	-1.748594E+02	-1.884805E+02	-1.374822E+01	
	3	-2.147266E+01	-1.833477E+02	-1.977344E+02	-3.789819E+01	
	4	1.852734E+01	-1.436172E+02	-9.144141E+01	-3.469116E+01	
	5	3.554688E+00	-1.594141E+02	-1.403945E+02	-2.421631E+01	
60	1	-1.393296E+04	-1.336465E+04	-1.249986E+04	-4.708750E+02	
	2	-1.382805E+04	-1.320893E+04	-1.124329E+04	-1.631373E+03	
	3	5.717605E+03	7.028355E+03	9.198676E+03	-5.699531E+02	
	4	1.053809E+04	1.194596E+04	1.286772E+04	-9.394531E+00	
	5	-2.877285E+03	-1.924309E+03	-1.201797E+02	-5.203945E+02	
61	1	4.779605E+03	6.187418E+03	-5.690273E+02	1.368125E+02	
	2	1.396676E+03	2.707488E+03	-8.833242E+02	-7.180183E+02	
	3	-3.698047E+01	2.527020E+03	-9.309141E+02	5.281328E+02	
	4	4.030715E+03	6.784340E+03	6.814063E+01	1.382965E+03	
	5	2.540590E+03	4.547285E+03	-5.806680E+02	3.325469E+02	
62	1	4.564766E+03	7.318328E+03	1.314078E+03	2.591875E+02	
	2	-1.003516E+02	2.463586E+03	-1.079098E+03	-1.479613E+02	
	3	-7.060704E+02	2.126492E+03	-1.292441E+03	4.006094E+02	
	4	3.983023E+03	7.025336E+03	1.124961E+03	8.078203E+02	
	5	1.932719E+03	4.727461E+03	1.426563E+01	3.298203E+02	
63	1	2.035156E+00	-1.688945E+02	-1.815078E+02	-1.374609E+01	
	2	3.100000E+01	-1.186211E+02	-6.316797E+01	-1.957657E+01	
	3	1.294531E+01	-1.322539E+02	-7.837500E+01	2.060791E+01	
	4	-1.415625E+01	-1.809000E+02	-1.938086E+02	2.643848E+01	
	5	8.085938E+00	-1.496211E+02	-1.289961E+02	3.432617E+00	
67	1	-1.266872E+04	-1.280191E+04	-1.074617E+04	-6.621250E+02	
	2	-1.217917E+04	-1.230373E+04	-9.142191E+03	-9.118494E+02	
	3	4.471770E+03	4.613395E+03	7.908016E+03	-4.654699E+02	
	4	7.746750E+03	7.848187E+03	1.006874E+04	-2.157148E+02	
	5	-3.157227E+03	-3.148637E+03	-4.779687E+02	-5.638320E+02	

Table 6. Maximum stresses for new cooling design

From Eq. (2)

$$\frac{da}{dN} = 2.07 \times 10^{-8} (K)^{3.5} (a)^{3.5/2},$$

$$\int_{0.078}^{0.288} a^{-1.75} da = 3.035 \times 10^{-3} N,$$

$$N = \left(-\frac{1}{0.75} a^{-0.75} \right) \left|_{0.078}^{0.288} \right. \frac{1}{3.035 \times 10^{-3}},$$

or

$$N = 1859 \text{ cycles}.$$

This more than meets the required life criteria of 800 cycles.

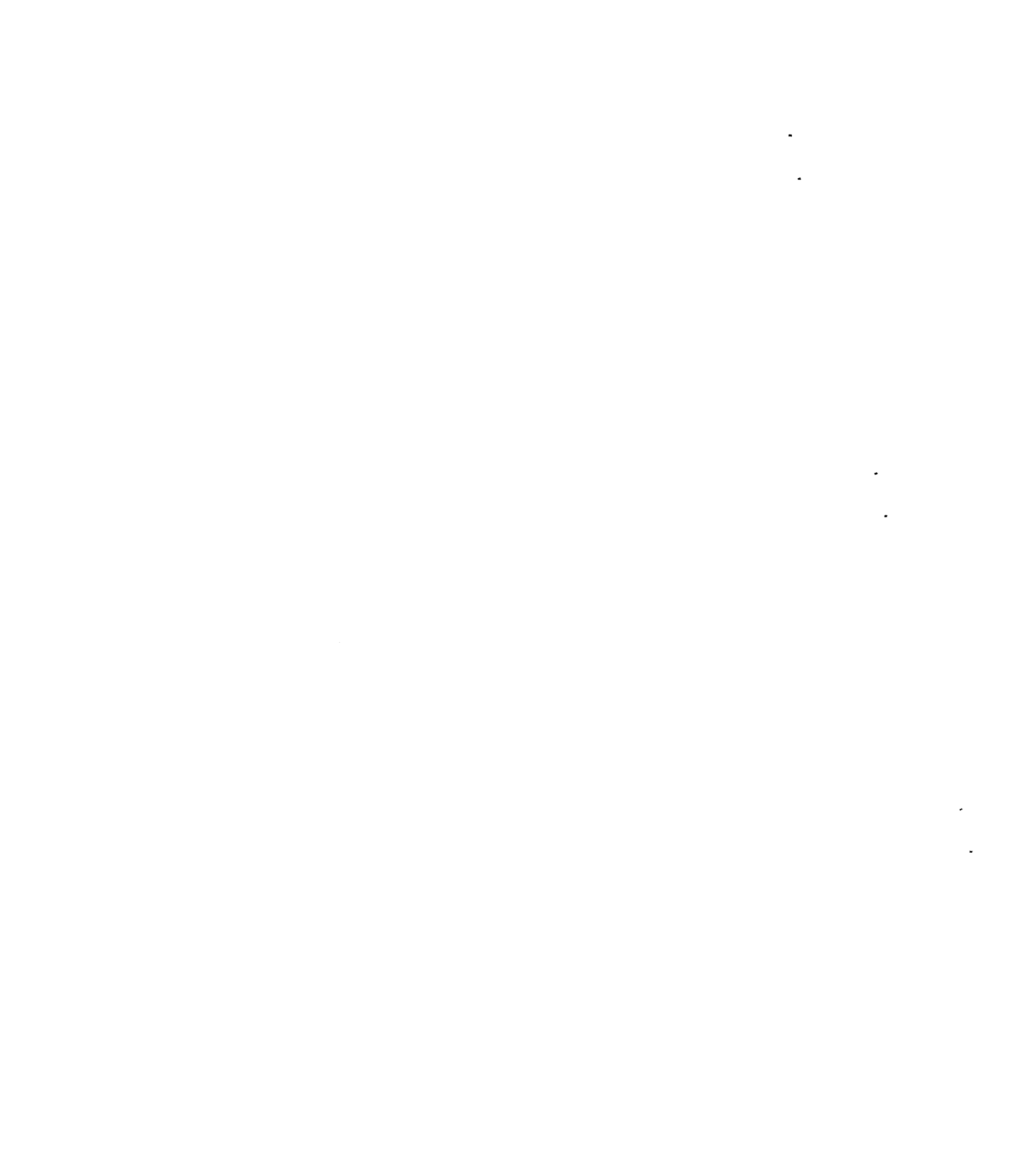
8. CONCLUSIONS

8.1 EPOXIED COOLING TUBES

This analysis shows that measured temperatures on EBT-S standard coils cannot exist unless the epoxy bond fails and allows a gap to develop between cooling tube and case. Such failure renders the cooling tube useless, and epoxy should not be used.

8.2 EFFECTS OF A NEW INTEGRALLY MACHINED COOLING SCHEME (Fig. 1)

With the designed cooling scheme, stresses would be reduced almost 60%, and the maximum flaw size could not grow to critical size, causing failure, in the planned lifetime of the machine.



Appendix A: THERMAL PROPERTIES

In order to find the amount of heat flowing from the coil and coil case to the cooling water for NASTRAN, several calculations had to be made. The first calculations were made to find the power generated by the copper conductor, with the average conductor temperature (T_{mc}) assumed to be 90°C. Therefore, the resistivity is $\rho_c = 0.88 \times 10^{-6} \Omega\text{-in.}$ (from Fig. A.1):

$$\dot{Q} = I^2 R , \quad (\text{A.1})$$

$$R = \frac{\rho_c L_c}{A_c} , \quad (\text{A.2})$$

where

$$L_{\text{cond}} = (16 \text{ paths})(287 \text{ cm/path})(1.0 \text{ in./2.54 cm})$$

$$L_{\text{cond}} = 1808 \text{ in.}$$

Using an EBT-S conductor, 0.444 in. \times 0.482 in. with a 0.217-in. inside diameter,

$$A_{\text{path}} = \frac{\pi(0.217 \text{ in.})^2}{4}$$

$$A_{\text{path}} = 0.036984 \text{ in.}^2$$

and

$$A_c = (0.444 \text{ in.})(0.482 \text{ in.}) - A_{\text{path}}$$

$$A_c = 0.1764255 \text{ in.}^2 .$$

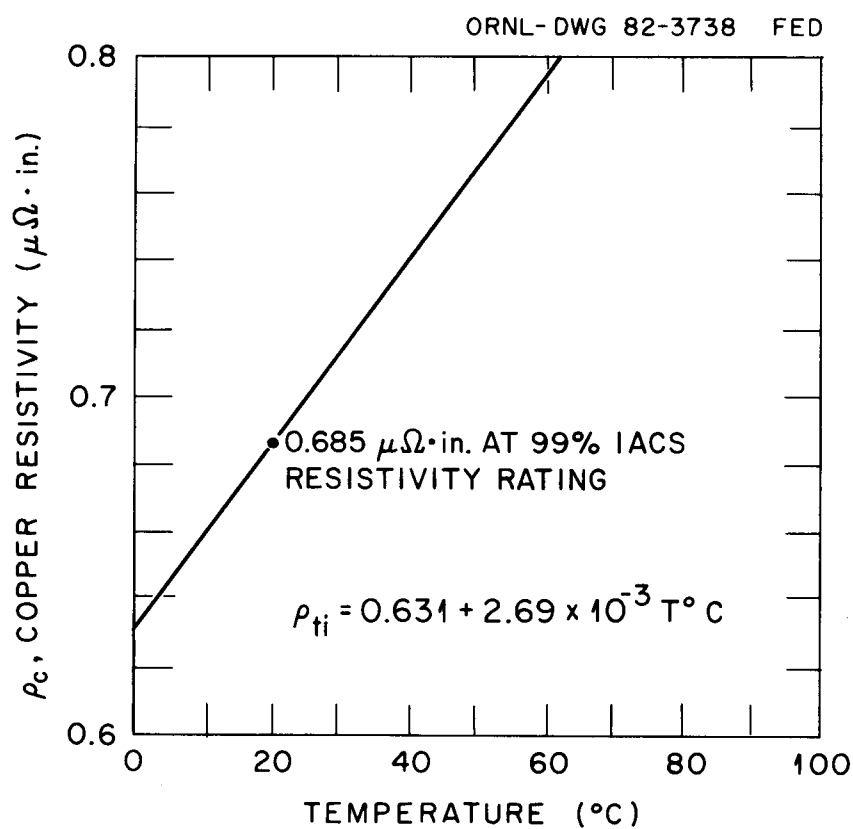


Fig. A.1. Temperature dependency of copper resistivity.

Therefore, from Eq. (2),

$$R = \frac{(0.88 \times 10^{-6} \Omega\text{-in.})(1808 \text{ in.})}{0.174255 \text{ in.}^2}$$

$$R = 9.018197 \times 10^{-3} \Omega .$$

At full power with $I = 9000 \text{ A}$, solving Eq. (A.2),

$$\dot{Q} = (9000 \text{ A})^2 (9.01897 \times 10^{-3} \Omega) \quad (\text{A.3})$$

$$\dot{Q} = 730,474 \text{ W/coil}$$

$$\dot{Q} = 692.82 \text{ Btu/s} .$$

For steady-state operation, the power generated by the coil must be removed by the cooling water:

$$\text{Inlet } P = 210 \text{ psig } (T = 80^\circ\text{F}) ,$$

$$\text{Exit } P = 40 \text{ psig} .$$

Using Bernoulli's equation, the velocity and mass flowrate of the water flowing in the conductor can be calculated. The heat removed by the water is

$$\dot{Q}_w = \dot{m} C_p \Delta T .$$

$$\Delta P = \frac{\rho}{2g} V^2 \left(f \frac{L}{D} + \Sigma K \right) ; \quad (\text{A.4})$$

Therefore,

$$V^2 = \frac{\Delta P 2g}{\rho (f \cdot L/D + \Sigma K)} . \quad (\text{A.5})$$

In order to find the velocity, the flow properties must be found:

$$L_{\text{cond}} = (287 \text{ cm})(1 \text{ in.}/2.54 \text{ cm})$$

$$L_{\text{cond}} = 113 \text{ in.} = 9.42 \text{ ft/cond.}$$

We need to add 6 ft more for the copper and nylon tubes. Therefore,

$$L_{\text{flow}} = 113 \text{ in.} + (6 \text{ ft})(12 \text{ in.}/1 \text{ ft}) = 185 \text{ in.}$$

The internal diameter of the conductor is

$$D = 0.217 \text{ in.}$$

The friction factor f is calculated from Prandtl's universal law of friction. Assuming turbulent flow $Re > 100,000$ and $f = 0.017$,

$$f_{\text{new}} = \left(\frac{1}{2[\log(\text{Re } \sqrt{f})] - 0.8} \right)^2. \quad (\text{A.6})$$

The loss coefficients (ΣK) for various transitions and fittings are:

	K	ΣK
2 elbows	0.9	1.8
Contraction	0.5	2.3
Expansion	1.0	3.3
4 Swageloks	0.05	3.5

The physical properties of the water must be known to find the velocity.

Assuming the bulk water temperature $T_b = 116.5^\circ\text{F}$, the bulk water properties are

$$C_p = 0.999 \text{ Btu/lbm} \cdot ^\circ \text{F} ,$$

$$\rho = 61.73 \text{ lbm/ft}^3 ,$$

$$K = 0.37 \text{ Btu/(h} \cdot \text{ft} \cdot ^\circ \text{F}) ,$$

$$v = 6.525 \times 10^{-6} \text{ ft/s, and}$$

$$\mu = 1.45 \text{ lbm/(h} \cdot \text{ft}) .$$

From Eq. (A.5)

$$V = \left(\frac{\Delta P 2g}{\rho (f \cdot L/D + \Sigma K)} \right)^{0.5} \quad (\text{A.7})$$

$$V = \left[\frac{(170 \text{ lbf/in.}^2)(2)(32.174 \text{ ft/s}^2)(144 \text{ in.}^2/\text{ft}^2)32.174(\text{lbm} \cdot \text{ft})/(1\text{bf} \cdot \text{s}^2)}{(61.73 \text{ lbm/ft}^3)(f \cdot 285/0.217 + 3.5)(32.174 \text{ ft/s}^2)} \right]^{0.5}$$

$$V = \left(\frac{255.83 \text{ ft}^2/\text{s}^2}{(f \cdot 852.54 + 3.5)} \right)^{0.5} \quad (\text{A.8})$$

Assuming $f = 0.017$, then $V = 37.674 \text{ ft/s}$. The Reynolds number Re calculations are

$$Re = \frac{\rho V D}{\mu} = \frac{(61.72 \text{ lbm/ft}^3)(V \cdot \text{ft/s})(0.217 \text{ in.})(1 \text{ ft}/12 \text{ in.})}{(1.45 \text{ lbm/h} \cdot \text{ft})(1 \text{ h}/3600 \text{ s})} , \quad (\text{A.9})$$

$$Re = V \left(\frac{2771.46}{\text{ft/s}} \right) , \quad (\text{A.10})$$

where $f = 0.017$ and $V = 37.674 \text{ ft/s}$; then $Re = 104,413$.

From Eq. (A.6), we calculate a new friction factor and use Eqs. (A.8) and (A.10) to iterate the final flow conditions:

$$f_{\text{new}} = 0.01791 ,$$

$$V = 36.88 \text{ ft/s , and}$$

$$Re = 102,121 .$$

Now, the mass flowrate can be found to calculate the heat removed by the water.

The mass flowrate for one of the 16 conductors is

$$\dot{m}/\text{path} = \rho V A_{\text{path}} = (61.73 \text{ lbm/ft}^3)(36.88 \text{ ft/s})(0.036984 \text{ in.}^2)(1 \text{ ft}^2/144 \text{ in.}^2)$$

$$\dot{m}/\text{path} = 0.5847 \text{ lbm/s} .$$

The overall mass flowrate for one coil is

$$\dot{m}_{\text{tot}} = (\dot{m}/\text{path})(16 \text{ paths}) = 9.3553 \text{ lbm/s} .$$

At steady-state operation the heat flow into the conductor is equal to the heat flow into the water:

$$\dot{Q}_{\text{water}} = \dot{Q}_{\text{cond}} , \quad (\text{A.11})$$

$$\dot{Q}_{\text{water}} = \dot{m}_{\text{tot}} C_p \Delta T . \quad (\text{A.12})$$

From Eq. (A.3),

$$\dot{Q}_{\text{cond}} = I^2 R = 692.82 \text{ Btu/s} . \quad (\text{A.13})$$

Substituting Eqs. (A.12) and (A.13) into (A.11),

$$\dot{m}_{\text{tot}} C_p \Delta T = 692.82 \text{ Btu/s}$$

with

$$\Delta T = \frac{692.82 \text{ Btu/s}}{\dot{m}_{\text{tot}} C_p}$$

$$\Delta T = \frac{692.82 \text{ Btu/s}}{(9.3553 \text{ lbm/s})(0.999 \text{ Btu/lbm} \cdot ^\circ\text{F})}$$

$$\Delta T = 74.130^\circ\text{F} ,$$

$$T_{\text{exit}} = T_{\text{in}} + \Delta T = 80^\circ\text{F} + 74.130^\circ\text{F} \quad (\text{A.14})$$

$$T_{\text{exit}} = 154.13^\circ\text{F} ,$$

and

$$T_{\text{bulk}} = \frac{T_{\text{in}} + T_{\text{exit}}}{2} = \frac{80^\circ\text{F} + 154.13^\circ\text{F}}{2} = 117.06^\circ\text{F} . \quad (\text{A.15})$$

The T_{bulk} assumed was 116.5°F , which is close enough to T_{bulk} calculated for the bulk water properties to remain constant.

In order to check the resistivity of the copper conductor, the temperature of the conductor must be calculated by using a bulk water temperature T_{bulk} of 116.5°F , and the final velocity and Reynolds number calculated. The heat-transfer coefficient must be calculated.

The Prandtl number Pr at the bulk temperature is

$$\text{Pr} = \frac{C_p \mu}{K} = \frac{(0.999 \text{ Btu/lbm} \cdot ^\circ\text{F})(1.45 \text{ lbm/h} \cdot \text{ft})}{(0.37 \text{ Btu/h} \cdot ^\circ\text{F} \cdot \text{ft})} \quad (\text{A.16})$$

$$\text{Pr} = 3.92 .$$

For turbulent heat-transfer coefficient the Dittus and Boelter equation is

$$h_c = 0.023 \frac{K}{D} (Re)^{0.8} (Pr)^{0.333} \quad (A.17)$$

$$h_c = 0.023 \frac{(0.37 \text{ Btu/h}\cdot\text{ft}\cdot{}^{\circ}\text{F})}{(0.217 \text{ in.})(1 \text{ ft}/12 \text{ in.})} (102121)^{0.8} (3.92)^{0.333}$$

$$h_c = 7741 \text{ Btu/h}\cdot\text{ft}^2\cdot{}^{\circ}\text{F} .$$

Using the heat transfer convection equation, the average temperature of the wall of the conductor can be calculated:

$$\dot{Q}_{\text{water}} = h_c A_s (T_{\text{wall}} - T_{\text{bulk}}) . \quad (A.18)$$

The surface area of the cooling passage in the conductor is

$$A_s = \pi D L_{\text{cond}} = \pi (0.217 \text{ in.})(1808 \text{ in.})(1 \text{ ft}^2/144 \text{ in.}^2)$$

$$A_s = 8.55944 \text{ ft}^2 .$$

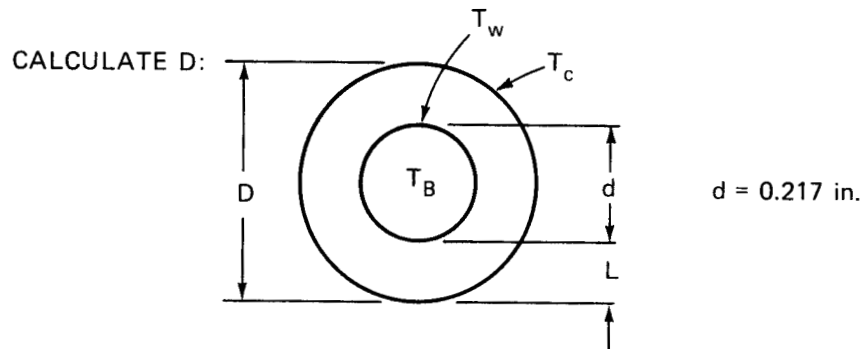
The temperature of the wall from Eq. (A.18) is

$$T_w = \frac{(692.82 \text{ Btu/s})(3600 \text{ s/h})}{(7741 \text{ Btu/h}\cdot\text{ft}^2\cdot{}^{\circ}\text{F})(8.55944 \text{ ft}^2)} + 116.5^{\circ}\text{F}$$

$$T_w = 154.14^{\circ}\text{F} = 67.856^{\circ}\text{C} .$$

The mean temperature of the copper conductor is needed to find the actual resistivity of the copper. To simplify this calculation, the conductor was assumed to be a circular tube with all of the I^2R heating flowing through the outside edge (see Fig. A.2).

ORNL-DWG 82-3782 FED



$$A = 0.1764255 \text{ in.}^2 = \frac{\pi D^2}{4} - \frac{\pi(0.217 \text{ in.})^2}{4}$$

$$D = \left(\frac{4}{\pi} (0.1764255 \text{ in.}) + \frac{4 \pi (0.217 \text{ in.})^2}{4} \right)^{0.5}$$

$$D = 0.42136 \text{ in.}$$

Fig. A.2. Simplified copper conductor.

The heat transferred through the tubular copper conductor is

$$\dot{Q} = \frac{A_s K_{Cu}}{L} (T_c - T_w) \quad (A.19)$$

where

$$T_w = 154.14^\circ F ,$$

$$K_{Cu} = 220.1 \text{ Btu/h}\cdot\text{ft}\cdot{}^\circ\text{F} ,$$

$$L = \frac{(0.42136 \text{ in.} - 0.217 \text{ in.})(1 \text{ ft}/12 \text{ in.})}{2}$$

$$L = 0.0085167 \text{ ft} ,$$

and

$$A_s = \pi D L_{cond}$$

$$A_s = \frac{\pi(0.42136 \text{ in.})(1808 \text{ in.})}{144 \text{ in.}^2/\text{ft}^2}$$

$$A_s = 16.62 \text{ ft}^2 .$$

From Eq. (A.19)

$$\dot{Q} = 692.82 \text{ Btu/s} = \frac{(16.62 \text{ ft}^2)(220.1 \text{ Btu/h}\cdot\text{ft}\cdot{}^\circ\text{F})}{0.0085167 \text{ ft}} (T_c - 154.44^\circ F)$$

$$\dot{Q} = \frac{(692.82 \text{ Btu/s})(0.0085167 \text{ ft})(3600 \text{ s/h})}{(16.62 \text{ ft}^2)(220.1 \text{ Btu/h}\cdot\text{ft}\cdot{}^\circ\text{F})}$$

$$\dot{Q} = 159.98^\circ F .$$

The highest temperature would occur if all heat is generated outside the conductor.

$$T_{mc} = \frac{T_c + T_w}{2} = \frac{154.14 + 159.98}{2} = 157.06^\circ F ,$$

$T_{mc} = 157.06^\circ F = 69.48^\circ C$, and from Fig. A.1 ,

$$\rho_c = 0.818 \times 10^{-6} \Omega \text{ in.} ,$$

$$\dot{Q} = \frac{\rho_c L_c}{A_c} I^2 = \frac{(0.818 \times 10^{-6} \Omega \text{ in.})(1808 \text{ in.})(9000^2)}{0.1764255 \text{ in.}^2}$$

$$\dot{Q} = 679,009 \text{ W/coil}$$

$$\dot{Q} = 644.007 \text{ Btu/s} .$$

After many iterations, the final flow properties for the conductor are found below:

$$V = 36.88 \text{ ft/s} ,$$

$$Re = 102,232 ,$$

$$\dot{m}_{\text{tot coil}} = 9.3553 \text{ lbm/s} ,$$

and

$$\dot{V}_{\text{tot coil}} = 68.0212 \text{ gal/min} .$$

Using new \dot{Q} , new $T_{exit} = 152^\circ F$, and new $T_b = 116^\circ F$,

$$h_c = 7741 \text{ Btu/h}\cdot\text{ft}^2\cdot{}^\circ\text{F}$$

$$T_w = 151^\circ F ,$$

$$T_c = 156.4^\circ F ,$$

$$T_{mc} = 153.7^\circ F = 67.61^\circ C ,$$

$$\rho_c = 0.810 \times 10^{-6} \Omega \text{ in.} ,$$

$$\dot{Q}_{\text{new}} = 637.70 \text{ Btu/s} = 672368 \text{ W/coil} .$$

Assuming the coil case will have maximum power input (200 kW/24 coils = 8.33 kW/coil), the heat transfer coefficient is needed to find the temperature in the coil case:

$$\dot{Q}_{\text{FLUX/COIL}} = 8330 \text{ W/coil} .$$

Flow properties and temperatures are needed for the coil case; using Eqs. (A.6), (A.7), and (A.9), the final flow properties are calculated. Calculating the flow properties we find

$$L = \pi D + \text{length to headers}$$

$$L = \pi(11.75 \text{ in.}) + 40 \text{ in.}$$

$$L = 77 \text{ in.}$$

The cooling channel area is (see Fig. A.3)

$$A = \frac{1}{2} \frac{\pi 0.25^2}{4} + (0.2 - 0.125)(0.25)$$

$$A = 0.043294 \text{ in.}^2 .$$

The hydraulic radius is

$$H_R = \frac{A}{\text{Perimeter}}$$

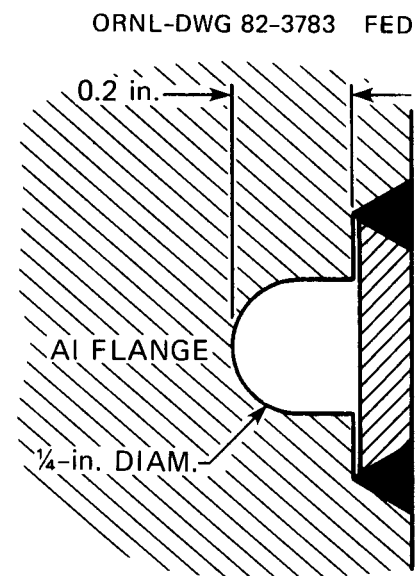


Fig. A.3. Case-cooling channel.

where

$$\text{Perimeter} = \frac{1}{2} (\pi)(0.25) + 0.25 + 2.0(0.2 - 0.125)$$

$$\text{Perimeter} = 0.7926911 \text{ in.}$$

$$H_R = \frac{0.043294 \text{ in.}^2}{0.7926911 \text{ in.}} \quad (\text{A.20})$$

$$H_R = 0.0546155 \text{ in.}^2$$

$$D_{\text{equ}} = 4H_R$$

$$D_{\text{equ}} = 0.2185 \text{ in.}$$

To find ΣK losses from fittings we take

	K	ΣK
4 elbows	0.90	3.6
Contraction	0.50	4.1
Expansion	1.00	5.1
2 Swageloks	0.05	5.2

$$\Sigma K = 5.2$$

Assuming the bulk water temperature $T_b = 85^\circ\text{F}$,

$$\rho = 62.17 \text{ lbm/ft}^3 ,$$

$$C_p = 0.9975 \text{ Btu/lbm} \cdot {}^\circ\text{F} ,$$

and

$$\mu = 1.969 \text{ lbm/ft} \cdot \text{h} .$$

The velocity was calculated using Eq. (A.7):

$$V = \left[\frac{(170 \text{ lbf/in.}^2)(2)(32.174 \text{ ft/s}^2)(144 \text{ in.}^2/1 \text{ ft}^2)(32.174 \text{ lbm-ft/lbf-s}^2)}{(62.17 \text{ lbm/ft}^3)(f 77/0.2185 + 5.2)(32.174 \text{ ft/s}^2)} \right]^{0.5} \quad (\text{A.21})$$

$$V = \left[\frac{25337.6}{(f350 + 5.2)} \right]^{0.5},$$

where

$$f = 0.016, \quad V = 48.44 \text{ ft/s};$$

$$Re = \frac{\rho V D}{\mu} = \frac{(62.17 \text{ lbm/ft}^3)(V \text{ ft/s})(0.2185 \text{ in.})(1 \text{ ft}/12 \text{ in.})}{(1.969 \text{ lbm/h ft})(1 \text{ h}/3600 \text{ s})}$$

$$Re = V \frac{2069.7}{\text{ft/s}}, \quad (\text{A.22})$$

where

$$f = 0.016 \text{ and } V = 52.48 \text{ ft/s, } Re = 100,248.$$

From Eq. (A.6), we calculate a new friction factor and use Eqs. (A.21) and (A.22) to iterate the final flow conditions:

$$f_{\text{new}} = 0.018094,$$

$$V = 46.87 \text{ ft/s, and}$$

$$Re = 97,010.$$

The mass flowrate for one cooling channel is

$$\dot{m} = \rho V A$$

$$= (62.17 \text{ lbm/ft}^3)(46.87 \text{ ft/s})(0.043294 \text{ in.}^2)(1 \text{ ft}^2/144 \text{ in.}^2)$$

$$\dot{m} = 0.876 \text{ lbm/s} ;$$

$$\dot{Q}_{\text{flux}} = \dot{Q}_{\text{water}}$$

= 4167 W/cooling channel at full power ,

$$Q_{\text{water}} = \dot{m} C_p \Delta T = 4167 \text{ W} = 3.9522 \text{ Btu/s} ;$$

$$\Delta T = \frac{\dot{Q}}{\dot{m}} = \frac{3.9522 \text{ Btu/s}}{(0.876 \text{ lbm/s})(0.9975 \text{ Btu/lbm}\cdot{}^{\circ}\text{F})} = 4.52 .$$

The exit temperature of the case cooling is

$$T_{\text{exit}} = T_{\text{in}} + \Delta T = 80 + 4.52$$

$$T_{\text{exit}} = 84.52^{\circ}\text{F}$$

and

$$T_{\text{bulk}} = [T_{\text{exit}} + T_{\text{in}}]/2$$

$$T_{\text{bulk}} = 82.26^{\circ}\text{F} \text{ (close enough to } T_{\text{bulk}} = 85^{\circ}\text{F}).$$

We find the film coefficient of the channel using $T_{\text{bulk}} = 85^{\circ}\text{F}$:

$$\rho = 62.17 \text{ lbm/ft}^3 ,$$

$$\mu = 0.547 \times 10^{-3} \text{ lbm/ft}\cdot\text{s} ,$$

$$K_A \text{ of Al} = 118 \text{ Btu/h}\cdot\text{ft}\cdot{}^{\circ}\text{F} ,$$

$$K_W \text{ of H}_2\text{O} = 0.353 \text{ Btu/h}\cdot\text{ft}\cdot{}^{\circ}\text{F} ,$$

$$C_p = 0.9975 \text{ Btu/lbm}\cdot{}^{\circ}\text{F} ,$$

and

$$\Pr = \frac{C_p \mu}{K} = \frac{(0.9975 \text{ Btu/lbm}\cdot{}^{\circ}\text{F})(0.547 \times 10^{-3} \text{ lbm/ft}\cdot\text{s})}{(0.353 \text{ Btu/h}\cdot\text{ft}\cdot{}^{\circ}\text{F})(1 \text{ h}/3600 \text{ s})} ,$$

$$\Pr = 5.56 .$$

Using Eq. (A.17)

$$h_c = 0.023 \frac{(0.353 \text{ Btu/h}\cdot\text{ft}\cdot{}^{\circ}\text{F})}{(0.2185 \text{ in.})(1 \text{ ft}/12 \text{ in.})} (97,010)^{0.8}(5.56)^{0.333}$$

$$h_c = 7705.4 \text{ Btu/h}\cdot\text{ft}\cdot{}^{\circ}\text{F} .$$

To calculate the temperature of the cooling channel we take

$$\dot{Q} = h_c A_s (T_{cc} - T_b) ,$$

$$\text{Length}_{cc} = \pi(11.75 \text{ in.}) ,$$

$$\text{Length}_{cc} = 37 \text{ in.} ,$$

and Eq. (A.20) ,

$$A_s = \text{Length}_{cc} \cdot \text{Perimeter}_{cc} = (0.7926911 \text{ in.})(37 \text{ in.})(1 \text{ ft}^2/144 \text{ in.}^2)$$

$$A_s = 0.2032 \text{ ft}^2 .$$

Thus,

$$\dot{Q} = 3.952 \text{ Btu/s} = (7705.4 \text{ Btu/h}\cdot\text{ft}^2\cdot{}^{\circ}\text{F})(0.2032 \text{ ft}^2)(T_{cc} - T_b)$$

and

$$T_{cc} = \frac{(3.952 \text{ Btu/s})(3600 \text{ s/h})}{1566.0 \text{ Btu/h}\cdot{}^{\circ}\text{F}} + 82.26^{\circ}\text{F}$$

$$T_{cc} = 9.08 + 82.26^{\circ}\text{F}$$

$$T_{cc} = 91.3^{\circ}\text{F} .$$

The cooling channel flow conditions are

$$T_{bulk} = 82.26^{\circ}\text{F} ,$$

$$V = 46.87 \text{ ft/s} ,$$

$m = 0.876 \text{ lbm/s}$,
 $\dot{V} = 6.3 \text{ gal/min}$,
 $h_c = 7705.4 \text{ Btu/h}\cdot\text{ft}^2\cdot{}^\circ\text{F}$,

and

$$T_{cc} = 91.3^\circ\text{F} .$$

Now all physical properties of the coil are established, and the properties are imputed into NASTRAN.

Appendix B: BASELINE NASTRAN INPUT

CARD COUNT	CASE C O N T R O L D E C K E C H O
1	TITLE#EBT MIRROR COIL HEAT LOADS TEMP-CONTOUR-PLOT
2	SUBTITLE#RIGID FORMAT #1
3	LABEL#RING ELEMENTS,HEAT FLOW
4	SPC#100
5	LOAD#9
6	OLOAD#ALL
7	THERMAL%PRINT,PUNCH<#ALL
8	PLOTID#RETURN TO C.HAMMONDS,BLDG.9204-1 MS 13
9	OUTPUT#PLOT<
10	PLOTTER NASTPLT MODEL D,1
11	PAPER SIZE 8.5 X 11.0
12	AXES Y,Z X
13	VIEW 0. 6. 0.
14	SET 100\$ALL EXCEPT ELEMENTS 200 THRU 229 EXCEPT,
15	GRID POINTS 148 THRU 150
16	MAXIMUM DEFORMATION#1
17	CONTOUR MAGNITUD LIST 228.,262.,296.,331.,365.,399.,434.,
18	468. Z1 COMMON
19	FIND SCALE ORIGIN 1 SET 100
20	PLOT CONTOUR
21	BEGIN BULK

*** USER INFORMATION MESSAGE 207, BULK DATA NOT SORTED,XSORT WILL RE-ORDER DECK.

CARD COUNT		S O R T E D	B U L K	D A T A	E C H O
51-	1	2	3	4	5 ..
52-	CHBDY	227	21	POINT	145
53-	&7Q2	150			
54-	CHBDY	228	21	POINT	146
55-	&7Q3	150			
56-	CHBDY	229	21	POINT	147
57-	&7Q4	150			
58-	CTRAPRG	1	1	8	9
59-	CTRAPRG	2	2	9	10
60-	CTRAPRG	3	3	10	11
61-	CTRAPRG	4	4	11	12
62-	CTRAPRG	5	5	12	13
63-	CTRAPRG	6	6	13	14
64-	CTRAPRG	8	8	14	15
65-	CTRAPRG	9	9	17	18
66-	CTRAPRG	16	14	18	19
67-	CTRAPRG	17	15	21	22
68-	CTRAPRG	19	17	22	23
69-	CTRAPRG	26	23	29	30
70-	CTRAPRG	29	25	26	27
71-	CTRAPRG	30	26	33	34
72-	CTRAPRG	31	27	34	35
73-	CTRAPRG	33	29	35	36
74-	CTRAPRG	37	33	43	44
75-	CTRAPRG	38	34	38	39
76-	CTRAPRG	39	35	39	40
77-	CTRAPRG	43	38	40	41
78-	CTRAPRG	44	39	47	48
79-	CTRAPRG	45	40	48	49
80-	CTRAPRG	46	41	49	50
81-	CTRAPRG	47	43	50	51
82-	CTRAPRG	51	47	52	53
83-	CTRAPRG	55	50	56	57
84-	CTRAPRG	56	52	60	61
85-	CTRAPRG	60	56	64	65
86-	CTRAPRG	61	57	65	66
87-	CTRAPRG	62	58	66	67
88-	CTRAPRG	63	60	68	69
89-	CTRAPRG	67	64	72	73
90-	CTRAPRG	68	65	73	74
91-	CTRAPRG	69	66	74	75
92-	CTRAPRG	70	68	76	77
93-	CTRAPRG	74	72	80	81
94-	CTRAPRG	75	73	81	82
95-	CTRAPRG	76	74	82	83
96-	CTRAPRG	77	76	84	85
97-	CTRAPRG	81	80	88	89
98-	CTRAPRG	82	81	89	90
99-	CTRAPRG	83	82	90	91
	CTRAPRG	84	84	92	93
				94	95
				96	97
				98	99

CARD COUNT		S O R T E D	B U L K	D A T A	E C H O							
	1	2	3	4	5	6	7	8	..	9	..	10
101-	CTRAPRG	89	89	97	98	90	0	..	5	6	..	7
102-	CTRAPRG	90	90	98	99	91	0	..	6	6	..	7
103-	CTRAPRG	91	96	100	101	97	0	..	5	6	..	7
104-	CTRAPRG	92	97	101	102	98	0	..	5	6	..	7
105-	CTRAPRG	93	98	102	103	101	0	..	5	6	..	7
106-	CTRAPRG	94	100	104	105	102	0	..	5	6	..	7
107-	CTRAPRG	95	101	105	106	103	0	..	5	6	..	7
108-	CTRAPRG	96	102	106	107	105	0	..	5	6	..	7
109-	CTRAPRG	97	104	108	109	109	0	..	5	6	..	7
110-	CTRAPRG	98	105	109	110	110	0	..	5	6	..	7
111-	CTRAPRG	99	106	110	111	107	0	..	5	6	..	7
112-	CTRAPRG	100	108	112	113	114	0	..	5	6	..	7
113-	CTRAPRG	101	109	113	114	115	0	..	5	6	..	7
114-	CTRAPRG	102	110	116	117	117	0	..	5	6	..	7
115-	CTRAPRG	103	112	117	118	118	0	..	5	6	..	7
116-	CTRAPRG	104	113	117	119	119	0	..	5	6	..	7
117-	CTRAPRG	105	114	118	120	121	0	..	5	6	..	7
118-	CTRAPRG	106	116	121	122	122	0	..	5	6	..	7
119-	CTRAPRG	107	117	121	123	119	0	..	5	6	..	7
120-	CTRAPRG	108	118	122	123	0	..	5	6	..	7	5
121-	CTRIARG	7	7	14	15	0	..	5	6	..	7	5
122-	CTRIARG	10	10	19	11	0	..	5	6	..	7	5
123-	CTRIARG	11	11	19	20	0	..	5	6	..	7	5
124-	CTRIARG	12	11	20	12	0	..	5	6	..	7	5
125-	CTRIARG	13	12	20	13	0	..	5	6	..	7	5
126-	CTRIARG	14	13	21	14	0	..	5	6	..	7	5
127-	CTRIARG	15	13	23	24	0	..	5	6	..	7	5
128-	CTRIARG	18	16	30	12 ⁴	0	..	5	6	..	7	5
129-	CTRIARG	20	18	30	31	0	..	5	6	..	7	5
130-	CTRIARG	21	124	31	19	0	..	5	6	..	7	5
131-	CTRIARG	22	21	25	22	0	..	5	6	..	7	5
132-	CTRIARG	23	21	25	26	0	..	5	6	..	7	5
133-	CTRIARG	24	22	25	27	0	..	5	6	..	7	5
134-	CTRIARG	25	22	27	28	0	..	5	6	..	7	5
135-	CTRIARG	27	24	32	33	0	..	5	6	..	7	5
136-	CTRIARG	28	25	36	37	0	..	5	6	..	7	5
137-	CTRIARG	32	28	36	19	0	..	5	6	..	7	5
138-	CTRIARG	34	18	12 ⁴	125	0	..	5	6	..	7	5
139-	CTRIARG	35	19	31	32	0	..	5	6	..	7	5
140-	CTRIARG	36	125	31	37	0	..	5	6	..	7	5
141-	CTRIARG	40	36	41	42	0	..	5	6	..	7	5
142-	CTRIARG	41	37	46	47	0	..	5	6	..	7	5
143-	CTRIARG	42	38	32	20	0	..	5	6	..	7	5
144-	CTRIARG	48	125	41	126	0	..	5	6	..	7	5
145-	CTRIARG	49	19	32	49	0	..	5	6	..	7	5
146-	CTRIARG	50	20	57	58	0	..	5	6	..	7	5
147-	CTRIARG	52	48	57	58	0	..	5	6	..	7	5
148-	CTRIARG	53	49	58	50	0	..	5	6	..	7	5
149-	CTRIARG	54	49	58	25	0	..	5	6	..	7	5
150-	CTRIARG	57	126	32	0	..	5	6	..	7	5	

CARD COUNT	S O R T E D										B U L K	D A T A	E C H O
	1	2	3	4	5	6	7	..	8	..	9	..	10
151-	CTRIARG	58	147	96	88	0	6	6					
152-	CTRIARG	59	21	126	25		6	6					
153-	CTRIARG	64	20	126	21		6	6					
154-	CTRIARG	65	30	44	127		6	6					
155-	CTRIARG	66	127	44	45		6	6					
156-	CTRIARG	71	31	127	45		6	6					
157-	CTRIARG	72	30	127	31		6	6					
158-	CTRIARG	73	31	45	128		6	6					
159-	CTRIARG	78	128	45	46		6	6					
160-	CTRIARG	79	32	128	46		6	6					
161-	CTRIARG	80	31	128	32		6	6					
162-	CTRIARG	85	32	46	129		6	6					
163-	CTRIARG	86	129	46	38		6	6					
164-	CTRIARG	87	87	147	88		6	6					
165-	CTRIARG	109	33	129	38		6	6					
166-	CTRIARG	110	32	129	33		6	6					
167-	CTRIARG	111	44	53	130		6	6					
168-	CTRIARG	112	130	53	54		6	6					
169-	CTRIARG	113	130	54	45		6	6					
170-	CTRIARG	114	44	130	45		6	6					
171-	CTRIARG	115	45	54	131		6	6					
172-	CTRIARG	116	131	54	55		6	6					
173-	CTRIARG	117	131	55	46		6	6					
174-	CTRIARG	118	45	131	46		6	6					
175-	CTRIARG	119	46	55	132		6	6					
176-	CTRIARG	120	132	55	56		6	6					
177-	CTRIARG	121	47	132	56		6	6					
178-	CTRIARG	122	46	132	47		6	6					
179-	CTRIARG	123	53	61	133		6	6					
180-	CTRIARG	124	133	61	62		6	6					
181-	CTRIARG	125	54	133	62		6	6					
182-	CTRIARG	126	53	133	63		6	6					
183-	CTRIARG	127	54	62	134		6	6					
184-	CTRIARG	128	134	62	63		6	6					
185-	CTRIARG	129	134	63	55		6	6					
186-	CTRIARG	130	54	134	55		6	6					
187-	CTRIARG	131	55	63	135		6	6					
188-	CTRIARG	132	135	63	64		6	6					
189-	CTRIARG	133	135	64	56		6	6					
190-	CTRIARG	134	55	135	56		6	6					
191-	CTRIARG	135	61	69	136		6	6					
192-	CTRIARG	136	136	69	70		6	6					
193-	CTRIARG	137	136	70	62		6	6					
194-	CTRIARG	138	61	136	62		6	6					
195-	CTRIARG	139	62	70	71		6	6					
196-	CTRIARG	140	137	70	63		6	6					
197-	CTRIARG	141	137	71	63		6	6					
198-	CTRIARG	142	62	137	63		6	6					
199-	CTRIARG	143	63	71	138		6	6					
200-	CTRIARG	144	138	71	72		0						

CARD COUNT			S O R T E D			B U L K		D A T A		E C H O	
	1	2	3	4	5	6	7	8	9	10	.
201-	CTRIARG	145	138	72	64	0	6
202-	CTRIARG	146	63	138	64	000	6	6	6	6	.
203-	CTRIARG	147	69	77	139	000	6	6	6	6	.
204-	CTRIARG	148	139	77	78	000	6	6	6	6	.
205-	CTRIARG	149	139	78	70	000	6	6	6	6	.
206-	CTRIARG	150	69	139	70	000	6	6	6	6	.
207-	CTRIARG	151	70	78	140	000	6	6	6	6	.
208-	CTRIARG	152	140	78	79	000	6	6	6	6	.
209-	CTRIARG	153	140	79	71	000	6	6	6	6	.
210-	CTRIARG	154	70	140	141	000	6	6	6	6	.
211-	CTRIARG	155	71	79	80	000	6	6	6	6	.
212-	CTRIARG	156	141	79	80	000	6	6	6	6	.
213-	CTRIARG	157	141	80	72	000	6	6	6	6	.
214-	CTRIARG	158	71	141	72	000	6	6	6	6	.
215-	CTRIARG	159	77	85	142	000	6	6	6	6	.
216-	CTRIARG	160	142	85	86	000	6	6	6	6	.
217-	CTRIARG	161	142	86	78	000	6	6	6	6	.
218-	CTRIARG	162	77	142	78	000	6	6	6	6	.
219-	CTRIARG	163	78	86	143	000	6	6	6	6	.
220-	CTRIARG	164	143	86	87	000	6	6	6	6	.
221-	CTRIARG	165	143	87	79	000	6	6	6	6	.
222-	CTRIARG	166	78	143	79	000	6	6	6	6	.
223-	CTRIARG	167	79	87	144	000	6	6	6	6	.
224-	CTRIARG	168	144	87	88	000	6	6	6	6	.
225-	CTRIARG	169	144	88	80	000	6	6	6	6	.
226-	CTRIARG	170	79	144	80	000	6	6	6	6	.
227-	CTRIARG	171	85	93	145	000	6	6	6	6	.
228-	CTRIARG	172	145	93	94	000	6	6	6	6	.
229-	CTRIARG	173	145	94	86	000	6	6	6	6	.
230-	CTRIARG	174	85	145	86	000	6	6	6	6	.
231-	CTRIARG	175	86	94	146	000	6	6	6	6	.
232-	CTRIARG	176	146	94	95	000	6	6	6	6	.
233-	CTRIARG	177	146	95	87	000	6	6	6	6	.
234-	CTRIARG	178	86	146	87	000	6	6	6	6	.
235-	CTRIARG	179	87	95	147	000	6	6	6	6	.
236-	CTRIARG	180	147	95	96	000	6	6	6	6	.
237-	GRID	1		4.30	.00	0.0					
238-	GRID	2		4.31	.00	.50					
239-	GRID	3		4.34	.00	1.015					
240-	GRID	4		4.37	.00	1.25					
241-	GRID	5		4.42	.00	1.53					
242-	GRID	6		4.48	.00	1.75					
243-	GRID	7		4.50	.00	2.045					
244-	GRID	8		4.63	.00	0.0					
245-	GRID	9		4.63	.00	.50					
246-	GRID	10		4.63	.00	1.015					
247-	GRID	11		4.63	.00	1.25					
248-	GRID	12		4.63	.00	1.53					
249-	GRID	13		4.63	.00	1.75					
250-	GRID	14		4.63	.00	2.045					

CARD COUNT		S O R T E D			B U L K		D A T A			E C H O		
		1	2 ..	3 ..	4 ..	5 ..	6 ..	7 ..	8 ..	9 ..	10 ..	
251-	GRID	15		4.63	.00		2.19					
252-	GRID	16		4.73	.00		2.41					
253-	GRID	17		4.797	.00		0.0					
254-	GRID	18		4.797	.00		.50					
255-	GRID	19		4.797	.00		1.015					
256-	GRID	20		4.797	.00		1.53					
257-	GRID	21		4.797	.00		2.045					
258-	GRID	22		4.797	.00		2.19					
259-	GRID	23		4.797	.00		2.41					
260-	GRID	24		4.84	.00		2.63					
261-	GRID	25		4.98	.00		2.045					
262-	GRID	26		4.98	.00		2.41					
263-	GRID	27		4.98	.00		2.63					
264-	GRID	28		4.98	.00		2.78					
265-	GRID	29		5.253	.00		0.0					
266-	GRID	30		5.253	.00		.50					
267-	GRID	31		5.253	.00		1.015					
268-	GRID	32		5.253	.00		1.53					
269-	GRID	33		5.253	.00		2.045					
270-	GRID	34		5.253	.00		2.41					
271-	GRID	35		5.253	.00		2.63					
272-	GRID	36		5.22	.00		2.78					
273-	GRID	37		5.33	.00		2.94					
274-	GRID	38		5.33	.00		2.045					
275-	GRID	39		5.33	.00		2.41					
276-	GRID	40		5.33	.00		2.63					
277-	GRID	41		5.33	.00		2.78					
278-	GRID	42		5.33	.00		3.00					
279-	GRID	43		5.709	.00		0.0					
280-	GRID	44		5.709	.00		.50					
281-	GRID	45		5.709	.00		1.015					
282-	GRID	46		5.709	.00		1.53					
283-	GRID	47		5.709	.00		2.045					
284-	GRID	48		5.709	.00		2.41					
285-	GRID	49		5.709	.00		2.63					
286-	GRID	50		5.709	.00		2.78					
287-	GRID	51		5.709	.00		3.00					
288-	GRID	52		6.165	.00		0.0					
289-	GRID	53		6.165	.00		.50					
290-	GRID	54		6.165	.00		1.015					
291-	GRID	55		6.165	.00		1.53					
292-	GRID	56		6.165	.00		2.045					
293-	GRID	57		6.165	.00		2.41					
294-	GRID	58		6.165	.00		2.78					
295-	GRID	59		6.165	.00		3.00					
296-	GRID	60		6.621	.00		0.0					
297-	GRID	61		6.621	.00		.50					
298-	GRID	62		6.621	.00		1.015					
299-	GRID	63		6.621	.00		1.53					
300-	GRID	64		6.621	.00		2.045					

CARD COUNT	S O R T E D B U L K D A T A E C H O									
	1	2 ..	3 ..	4 ..	5 ..	6 ..	7 ..	8 ..	9 ..	10 ..
301-	GRID 65		6.621	.00	2.41					
302-	GRID 66		6.621	.00	2.78					
303-	GRID 67		6.621	.00	3.00					
304-	GRID 68		7.077	.00	0.0					
305-	GRID 69		7.077	.00	.50					
306-	GRID 70		7.077	.00	1.015					
307-	GRID 71		7.077	.00	1.53					
308-	GRID 72		7.077	.00	2.045					
309-	GRID 73		7.077	.00	2.41					
310-	GRID 74		7.077	.00	2.78					
311-	GRID 75		7.077	.00	3.00					
312-	GRID 76		7.533	.00	0.0					
313-	GRID 77		7.533	.00	.50					
314-	GRID 78		7.533	.00	1.015					
315-	GRID 79		7.533	.00	1.53					
316-	GRID 80		7.533	.00	2.045					
317-	GRID 81		7.533	.00	2.41					
318-	GRID 82		7.533	.00	2.78					
319-	GRID 83		7.533	.00	3.00					
320-	GRID 84		7.989	.00	0.0					
321-	GRID 85		7.989	.00	.50					
322-	GRID 86		7.989	.00	1.015					
323-	GRID 87		7.989	.00	1.53					
324-	GRID 88		7.989	.00	2.045					
325-	GRID 89		7.989	.00	2.41					
326-	GRID 90		7.989	.00	2.78					
327-	GRID 91		7.989	.00	3.00					
328-	GRID 92		8.445	.00	0.0					
329-	GRID 93		8.445	.00	.50					
330-	GRID 94		8.445	.00	1.015					
331-	GRID 95		8.445	.00	1.53					
332-	GRID 96		8.445	.00	2.045					
333-	GRID 97		8.445	.00	2.41					
334-	GRID 98		8.445	.00	2.78					
335-	GRID 99		8.445	.00	3.00					
336-	GRID 100		8.81	.00	2.045					
337-	GRID 101		8.81	.00	2.41					
338-	GRID 102		8.81	.00	2.78					
339-	GRID 103		8.81	.00	3.00					
340-	GRID 104		9.31	.00	2.045					
341-	GRID 105		9.31	.00	2.41					
342-	GRID 106		9.31	.00	2.78					
343-	GRID 107		9.31	.00	3.00					
344-	GRID 108		9.81	.00	2.045					
345-	GRID 109		9.81	.00	2.41					
346-	GRID 110		9.81	.00	2.78					
347-	GRID 111		9.81	.00	3.00					
348-	GRID 112		10.31	.00	2.045					
349-	GRID 113		10.31	.00	2.41					
350-	GRID 114		10.31	.00	2.78					

CARD COUNT			S O R T E D			B U L K		D A T A		E C H O							
	1	2	3	..	4	..	5	..	6	..	7	..	8	..	9	..	10
401-	PHBDY	11	25		.00												
402-	PHBDY	12	26		.00												
403-	PHBDY	13	27		.00												
404-	PHBDY	14	29		1.00												
405-	PHBDY	15	30		1.00												
406-	PHBDY	16	31		1.00												
407-	PHBDY	17	32		1.00												
408-	PHBDY	18	33		1.00												
409-	PHBDY	19	34		1.00												
410-	PHBDY	20	35		1.00												
411-	PHBDY	21	36		1.00												
412-	PHBDY	22	28		.00												
413-	QHBDY	9	LINE			27.02		1	24					2	28		
414-	QHBDY	9	LINE		.39000	30.08		28						3	37		
415-	QHBDY	9	LINE		.39000	31.30		37						4	42		
416-	QHBDY	9	LINE		.39000	33.00								5			
417-	HBDY	9	LINE		.00	27.08		2	3					6			
418-	HBDY	9	LINE		.00	27.26		4	4					7			
419-	HBDY	9	LINE		.00	27.46		5	5					8			
420-	HBDY	9	LINE		.00	27.78		6	6					9			
421-	HBDY	9	LINE		.00	28.14		7	7					10			
422-	HBDY	9	LINE		.00	28.66		15	15					11			
423-	HBDY	9	LINE		.00	29.10		16	16					12			
424-	HBDY	9	LINE		.00	29.72		42	42					13			
425-	HBDY	9	LINE		.00	33.48		51	51					14			
426-	HBDY	9	LINE		.00	35.88		59	59					15			
427-	HBDY	9	LINE		.00	38.74		67	67					16			
428-	HBDY	9	LINE		.00	41.60		75	75					17			
429-	HBDY	9	LINE		.00	44.46		83	83					18			
430-	HBDY	9	LINE		.00	47.34		91	91					19			
431-	HBDY	9	LINE		.00	50.20		99	99					20			
432-	HBDY	9	LINE		.00	53.06		103	103					21			
433-	HBDY	9	LINE		.00	55.36		107	107					22			
434-	HBDY	9	LINE		.00	58.50		107	107					23			
435-	HBDY	9	LINE		-.00027253.06	92								24			
436-	HBDY	9	LINE		-.00027253.06	93								25			
437-	HBDY	9	LINE		-.00027253.06	94								26			
438-	HBDY	9	LINE		-.00027253.06	95								27			
439-	HBDY	9	LINE		-.00027253.06	96								28			
440-	HBDY	9	LINE		-.00027255.36	100								29			
441-	HBDY	9	LINE		-.00027258.50	104								30			
442-	HBDY	9	LINE		-.00027261.64	108								31			
443-	HBDY	9	LINE		-.00027261.64	111								32			
444-	HBDY	9	LINE		-.00027264.78	112								33			
445-	HBDY	9	LINE		-.00027264.78	115								34			
446-	HBDY	9	LINE		-.00027267.92	116								35			
447-	HBDY	9	LINE		-.00027269.86	120								36			
448-	HBDY	9	LINE		-.00027269.86	121								37			
449-	HBDY	9	LINE		-.00027269.86	122								38			
450-	HBDY	9	LINE		-.00173067.92	119								39			

CARD		S	O	R	T	E	D	B	U	L	K	D	A	T	A	E	C	H	O													
COUNT		1	.	9	2	.	1.226	3	.	20	4	.	21	5	.	22	6	.	28	7	.	34	8	.	35	9	.	X	Z	Y	10	.
451-	QVOL							36		48			49			50			57			58			59			64ZPR				
452-	EYZ							65		66			71			72			73			78			79			80GHI				
453-	SPR							85		86			87																			
454-	EHI																															
455-	QVOL	9						1.226		109			THRU			180																
456-	SPC	50						148					100																			
457-	SPC	51						149					128.0																			
458-	SPC	52						150					159.0																			
459-	SPCADD	100						50		51			52																			
460-	SPOINT	148																														
461-	SPOINT	149																														
462-	SPOINT	150																														
	ENDDATA																															

ORNL/TM-8364
Dist. Category UC-20

INTERNAL DISTRIBUTION

- | | |
|----------------------|--|
| 1-5. J. A. Mayhall | 27. R. V. Lunsford |
| 6-10. G. A. Byington | 28. W. D. Shipley |
| 11. J. W. Forseman | 29. J. E. Warwick |
| 12. C. J. Hammonds | 30. K. K. Chipley |
| 13. G. R. Haste | 31. B. E. Nelson |
| 14. R. L. Johnson | 32. T. J. McManamy |
| 15. J. L. Livingston | 33. W. E. Bryan |
| 16. J. Sheffield | 34. O. B. Morgan |
| 17. R. P. Donaldson | 35-36. Laboratory Records Department |
| 18. R. G. Clark | 37. Laboratory Records, ORNL-RC |
| 19. C. C. Queen | 38. Document Reference Section |
| 20. T. L. Ryan | 39-40. Central Research Library |
| 21. D. J. Taylor | 41. Fusion Energy Division
Library |
| 22. E. H. Bryant | 42. Fusion Energy Division
Reports Office |
| 23. W. R. Hamilton | 43. ORNL Patent Office |
| 24. R. B. Wysor | |
| 25. L. A. Berry | |
| 26. R. L. Livesey | |

EXTERNAL DISTRIBUTION

44. J. D. Callen, Department of Nuclear Engineering, University of Wisconsin, Madison, WI 53706
45. R. W. Conn, Department of Chemical, Nuclear, and Thermal Engineering, University of California, Los Angeles, CA 90024
46. S. O. Dean, Director, Fusion Energy Development, Science Applications, Inc., 2 Professional Drive, Suite 249, Gaithersburg, MD 20760
47. H. K. Forsen, Bechtel Group, Inc., Research Engineering, P.O. Box 3965, San Francisco, CA 94105
48. R. W. Gould, Department of Applied Physics, California Institute of Technology, Pasadena, CA 94105
49. D. G. McAlees, Exxon Nuclear Company, Inc., 777 106th Avenue, NE, Bellevue, WA 98009
50. P. J. Reardon, Princeton Plasma Physics Laboratory, P.O. Box 451, Princeton, NJ 08540
51. W. M. Stacey, School of Nuclear Engineering, Georgia Institute of Technology, Atlanta, GA 30332
52. Bibliothek, Institut fur Plasmaphysik, D-8046 Garching bei Munchen, Federal Republic of Germany
53. Bibliothek, Institut fur Plasmaphysik, KFA, Postfach 1913, D-5170, Julich 1, Federal Republic of Germany
54. Bibliotheque, Service du Confinement des Plasmas, CEA, B.P. No. 6, 92 Fontenay-aux-Roses (Seine), France

55. Documentation S.I.G.N., Department de la Physique du Plasma et de la Fusion Controlee, Association EURATOM-CEA, Centre d'Etudes Nucleaires, B.P. 85, Centre du Tri, 38041 Grenoble, Cedex, France
 56. Library, Centre de Recherches en Physique des Plasmas, 21 Avenue des Bains, 1007 Lausanne, Switzerland
 57. Library, Culham Laboratory, UKAEA, Abingdon, Oxon, OX14 3DB, England
 58. Library, FOM Institute voor Plasma-Fusica, Rijnhuizen, Jutphaas, Netherlands
 59. Library, Institute for Plasma Physics, Nagoya University, Nagoya 464, Japan
 60. Library, International Centre for Theoretical Physics, Trieste, Italy
 61. Library, Laboratoria Gas Ionizzati, Frascati, Italy
 62. Plasma Research Laboratory, Australian National University, P.O. Box 4, Canberra, ACT 2000, Australia
 63. Thermonuclear Library, Japan Atomic Energy Research Institute, Tokai, Naka, Ibaraki, Japan
 64. Library, Plasma Physics Laboratory, Kyoto University, Gokasho Uji, Kyoto, Japan
 65. R. Varma, Physical Research Laboratory, Navangpura, Ahmedabad, India
 66. Institute of Physics, Academia Sinica, Peking, Peoples Republic of China
 67. Office of the Assistant Manager for Energy Research and Development, Department of Energy, Oak Ridge Operations, Oak Ridge, TN 37830
- 68-175. Given distribution as shown in TID-4500, Magnetic Fusion Energy (Distribution Category UC-20)